THESIS FOR THE DEGREE OF MASTER OF SCIENCE IN ENGINEERING PHYSICS

Vehicle Detection using Anisotropic Magnetoresistors

Martin Isaksson

CHALMERS

Report no. EX034/2008

Communication Systems
Department of Signals and Systems
CHALMERS UNIVERSITY OF TECHNOLOGY
Göteborg, Sweden, 2007

Vehicle Detection using Anisotropic Magnetoresistors

Master's Thesis EX034/2008

Communication Systems
Department of Signals and Systems
Chalmers University of Technology
SE-412 96 Göteborg
Sweden

Telephone +46 - (0)31 - 772 1000

Typeset in LaTeX2e
Göteborg, Sweden 2007

Vehicle Detection using Anisotropic Magnetoresistors
Martin Isaksson
Communication Systems
Department of Signals and Systems
Chalmers University of Technology

Abstract

A Wireless Sensor Network (WSN) of anisotropic magnetoresistor sensors offers a low-cost alternative to other traffic measurement technologies. The WSNs offer better reliability than other solutions, they offer more information, can be deployed quickly and be reused. In this thesis the sensor algorithms used for detection, velocity estimation, queue detection and classification in such a network are evaluated based on simulated and measured data. A number of algorithms are evaluated and the results are compared. A new algorithm for speed estimation using two sensor nodes is proposed and evaluated. It is found to be much better than earlier algorithms, requiring a signal to noise ratio (SNR) of 20 dB less than the traditional algorithm.

Keywords: Wireless Sensor Network, Anisotropic Magnetoresistor, Vehicle Detection, Vehicle Classification

Vehicle Detection using Anisotropic Magnetoresistors
Martin Isaksson
Communication Systems
Department of Signals and Systems
Chalmers University of Technology

Sammanfattning

Ett trådlöst sensornätverk (Wireless Sensor Network, WSN) av anisotropiska magnetoresistorsensorer erbjuder ett lågkostnadsalternativ till andra trafikmätningsmetoder. De ger bättre tillförlitlighet än andra metoder, de ger mer information, kan installeras snabbt och kan återanvändas. I det här examensarbetet utvärderas sensoralgoritmer för detektion, hastighetsestimering, ködetektion och klassificering i ett sådant nätverk baserat på simuleringar och mätdata. Ett antal algoritmer utvärderas och jämförs. En ny algoritm för hastighetsestimering förelås och evalueras. Det visas att den är bättre än föregående algoritmer och fordrar ett signal till brus-förhållande (SNR) på 20 dB mindre än tidigare algoritmer.

Nyckelord: Trådlösa sensornätverk, anisotropisk magnetoresistor, fordonsdetektion, fordonsklassificering

Preface

This thesis is part of a bigger Intelligent Transportation System (ITS) project undertaken by the two closely related companies – Qamcom Technology AB[1] and Amparo Solutions AB[2]. The goal of this project is to develop a traffic information system capable of delivering information in real-time to drivers, authorities and road maintenance personnel. The wireless sensor network proposed is evaluated in this project for different applications in an intelligent transportation system.

Acknowledgements

In the course of preparing this masters thesis I have realised that I am in debt to numerous people whose help I could not have done without. I would therefore like to thank everyone at Qamcom Technology AB, Amparo Solutions AB, Mantra Communication AB for their interest in my work – a heartfelt thanks to my advisers Patrik Bohlin and Henrik Linell. My examiner Professor Erik Ström should not only be credited for all his help during this thesis, but also for introducing me to the deeper realms of communication systems.

A mathematician named Alfréd Rényi once stated that "a mathematician is a device for turning coffee into theorems". Alfréd's theorem is equally true for physicists and engineers though the output might differ. During this thesis I have consumed an estimated 300 cups or 60 litres of coffee and for that I would like to thank everyone in the coffee making chain, from the coffee bean pickers in the highlands of Kenya to the employees at Qamcom. Without any single one of them, this thesis would still be in the process of being written.

I would also like to express my deep gratitude to all the researchers in this field for making their work available to me, through publications and Internet. My family has supported me through all of my studies – for that I am really thankful. Lastly I'd like to send my gratitude to those who have proofread my work – you have all given me a severe headache.

Göteborg, April 3, 2008

Martin Isaksson

[1] Qamcom Technology AB, `http://www.qamcom.se`
[2] Amparo Solutions AB, `http:///www.amparosolutions.se`

Contents

List of Figures

List of Tables

Definitions

- **Queue** – a line of people, vehicles or other objects. The first are dealt with first, so it is said to have a first-in first-out order, *FIFO*.
- **Up-time** – arrival of a vehicle.
- **Down-time** – departure of a vehicle.
- **On-time** – time between arrival and departure of a vehicle.

In this thesis the magnetic field strength refers to the magnetic field strength *relative* to the earth magnetic field strength unless otherwise stated. The measured quantity is the disturbance of the earth magnetic field so this notation is applicable.

Abbreviations and acronyms

AMR	Anisotropic Magnetoresistance
AP	Access Point
AVI	Automatic Vehicle Identification
AWGN	Additive White Gaussian Noise
DFT	Discrete Fourier Transform
FFD	Full-function Device
FFT	Fast Fourier Transform
FIFO	First-In First-Out
GPS	Global Positioning System
ISM	Industrial, Scientific and Medical
ITS	Intelligent Transportation System
LR-WPAN	Low-Rate Wireless Personal Area Networks
KLT	Karhunen-Loève Transform
MAC	Medium Access Control
PHY	Physical Layer
radar	Radio detection and ranging
RF	Radio Frequency
RFD	Reduced-function Device
RSSI	Received Signal Strength Indication
RX	Receive or receiver
SN	Sensor Node
SNR	Signal-to-Noise Ratio
S/R	Set/Reset
SUV	Sports Utility Vehicle
ToF	Time of Flight
TRX	Transceiver
TX	Transmit or transmitter
VIP	Video Image Processing

WIM	Weigh In Motion
WLAN	Wireless Local Area Network
WPAN	Wireless Personal Area Network
WSN	Wireless Sensor Networks

Notation

In the thesis, matrices and vectors are set in boldface, with upper-case letters for matrices and lower-case letters for vectors. The meaning of the following symbols – except where otherwise stated – are

$x[k], \quad k = 0, 1, \ldots, n$	kth sample of signal x
$\hat{\theta}$	An estimate of the parameter θ
$E[\cdot]$	Expectation of a variable
∇	Gradient
$\lvert\boldsymbol{u}\rvert$	Length (norm)
$\boldsymbol{B}, B$	Magnetic flux density [T = Vs/m^2]
$\mathbb{R}^n$	n-dimensional Euclidean space
μ_0	Permeability in vacuum
$\boldsymbol{u} \cdot \boldsymbol{v}$	Scalar product
$\boldsymbol{A}^T$	Transpose operator
$\hat{\boldsymbol{r}}$	Unit vector
$\boldsymbol{u} \times \boldsymbol{v}$	Vector product

Chapter 1

Introduction

1.1 Background

During the last decades the number of vehicles on our roads has increased exponentially. Personal mobility has increased from 17 km a day in 1970 to 35 km in 1998 and is nowadays taken for granted and seen as an acquired right [1]. This increased mobility has resulted in an increase of traffic congestion, pollution and accidents. The increased mobility and the demands of improved traffic safety mean an increased need of correct and in real-time available information.

The notion that a traffic system in the future will be based on real time communication between human–vehicle–infrastructure is not very far-fetched. A hypothesis is that the infrastructure will go from being static to being dynamic [2] which also means that the demand for information about traffic situations will increase.

If information about the current and future traffic situation can be forwarded from the infrastructure to the vehicle, then information about the best route can be shown to the driver. Getting to the desired destination within the specified time is however not the only benefit of such a system. The infrastructure of today was often planned many hundred of years ago with the national and international politics of the era in mind [1]. The roads were then widened to accommodate the traffic of the modern era. This spells trouble – the roads cannot withstand the traffic intensity, resulting in queues and even accidents. Real-time information, and even predictions about future traffic situations will mean that traffic is spread out on the existing road network and thus reducing the load on any single road.

In order to make predictions about the future, one must first have information about the present. A Wireless Sensor Network (WSN) can give such information. We propose a WSN made up out of many sensor nodes (SNs), equipped with magnetic sensors. These SNs are cheap, easy to install and give detailed information about each passing vehicle. In its simplest form it can not do a lot, but its strength comes from the network of SNs. There is also a choice to implement more computational power in each sensor node.

1.2 Purpose

The purpose of this thesis is to evaluate the use of a Wireless Sensor Network for traffic surveillance in a number of fields including detection, speed estimation, classification and queue detection. In each of these fields a number of algorithms will be evaluated for use in the system. One of the main goals is to develop a simulator for cheap and easy testing of the system. The simulator should accurately portrait the model described in Chapter 4 and therefore be able to be used for simulation of the algorithms found in this thesis.

The main questions to answer are whether a WSN is suitable for

- **traffic monitoring**, i.e., primarily counting, speed estimation and classification,
- **queue detection**, i.e., speed estimation and presence,

and what features of the sensor nodes and the algorithms used are needed for these applications. The thesis should investigate the performance of some algorithms for each case stated above and give specifications for the hardware. The applications can be both permanent and temporary in the sense that a pair of nodes can be placed permanently on-site or temporarily. The first application for our system will be replacing the old technology based on pneumatic tubes and provide statistics and queue detection.

1.3 Delimitations

This thesis is limited to the sensor part of the Wireless Sensor Network. This means that it is assumed that the network exists and works ideally except where otherwise stated. There are a number of delimitations in the models themselves. The delimitations will be covered in later chapters.

Figure 1.1: *During the last decades the number of vehicles on our roads has increased exponentially.*

Chapter 2

Method

This chapter aims to describe the scientific reasoning that forms the basis for the work done in this project. As an introduction, the work process is outlined. Thereafter the methods chosen are described. Finally a discussion about generality and validity follows.

2.1 Assault approach

Traditionally a completely deductive[1] assault approach has been used – one made observations, noted them with more or less readable handwriting in a notebook and made conclusions from that. The method used to find the relation to real world data by Imego can be said to be strictly deductive. The result has then been used to develop the model used in this thesis. The model has in its turn been used to develop the algorithms for use in the Wireless Sensor Network (WSN) that we propose, and we assume that they apply to real world situations. This method can be said to be inductive[2].

2.1.1 Description

The project is divided into parts. A short description of these parts now follows.

- A study of sensor networks, ad-hoc networks and previous work. Previous work include theses within the same project.
- Simulation of magnetic model and sensor model in MATLAB and other tools based on the magnetic model developed by IMEGO AB[3],
- Implementation, evaluation and improvement of algorithms in the simulator,
- Implementation in hardware made by a previous thesis project at Qamcom Technology AB,
- Verification of the model by field trials.

[1] *deductive*, "based on deduction from accepted premises: *deductive argument; deductive reasoning.*" `http://www.dictionary.com`

[2] *inductive*, "of, pertaining to, or employing logical induction: *inductive reasoning.*" `http://www.dictionary.com`

[3] `http://www.imego.se`

2.1.2 Discussion

The usage of a model to develop algorithms is an inductive approach, but this thesis has not been written solely by using this approach. Throughout the projects, we have used measurements to get more data for use in the model, an approach that can be said to be deductive. These measurements have been the foundation for the model developed, and the model has then been the basis for further studies. This approach is entirely inductive – therefore a combined inductive and deductive approach has been used. In this case these approaches has the benefit of being cheap, time effective and non-destructive as opposed to only doing field trials which are time consuming and costly since hardware must be rebuilt if they don't meet specifications and demands.

2.2 Procedure

In order to get acquainted with the Wireless Sensor Networks and the algorithms used today, the literature in this field have been studied. Using this as a basis, along with the study made by Imego AB, a simulator for the sensor system has then been developed. The simulator has been used to evaluate algorithms for the different applications.

2.3 Validity

The validity of the model used in this thesis can be discussed. It is proved empirically that it is valid at least in a small geographic area and its validity anywhere else in the world is assumed and inductively proved. The model should be iterative – one should go back and revise the model after simulations and field trials if the results do not match in order to increase validity. The downside of basing decisions on a model is of course not knowing if the model matches reality and therefore the results may not be valid. The validity is of course also determined by model parameters such as number of magnetic dipoles moments considered.

2.4 Generality

The basis of the model applies to a lot of similar projects, where you want to simulate real events because they may be expensive, destructive or time consuming. The model itself applies to similar detection applications with magnetic sensors, but the more specific algorithms can not be applied anywhere else.

Regarding the scope of this thesis, it can be said that since we do not have data from every vehicle on the market, we cannot say that our model is valid for all of those vehicles. However when we add more data, we do not change anything, and using the same methods discussed in this thesis, the model can be expanded to fit those vehicles.

Chapter 3

Wireless Sensor Networks

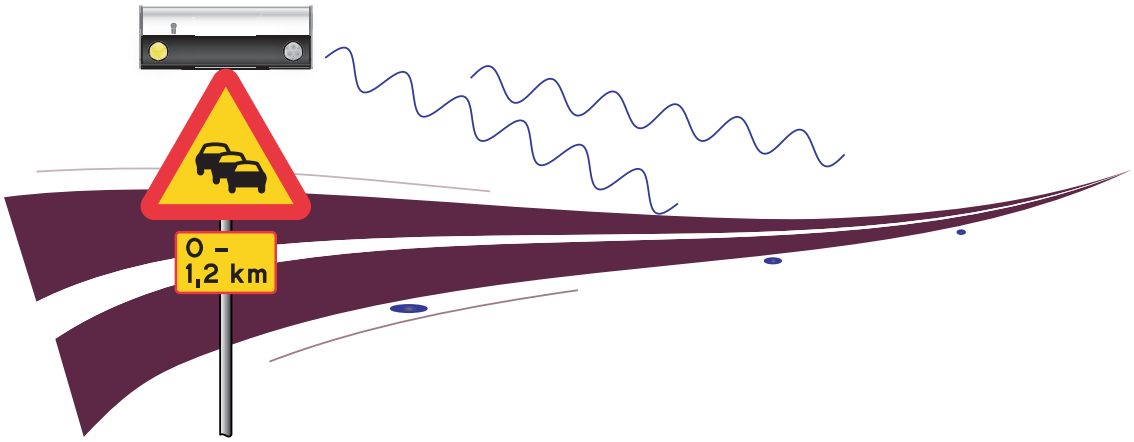

Figure 3.1: *Wireless Sensor Network together with a queue warning sign fitted with Amparo SeeMe™ flashing unit.*

3.1 "Ambient Intelligence" or putting electronics into groceries

There has been a tendency for some time now to put embedded computational power into large things such as washing machines and refrigerators. That tendency is not limited to large appliances but even disposable goods, groceries, living spaces and working spaces will soon be or already are endowed with such capabilities [3]. Computational power that surrounds us in our daily lives can be – somewhat praisefully – called "Ambient Intelligence" wherein many different devices will work together to control processes or interact with us. We should take this technology for granted, it should be unobtrusive and even invisible.

In the light of this, a new type of network emerged – the Wireless Sensor Network (WSN). Each individual node in the network is capable of sensing or interacting with its environment. However, it is first when they are connected to each other that they show their true power. WSNs have many applications and the technical solutions are very different.

An interesting example of a WSN is the "Smart Dust" proposed by the U.S. Defence Advanced Projects Agency (DARPA). The smart-dust sensor nodes are extremely small - about the size of a grain of sand or even a dust-particle. The idea is to scatter thousands of these small sensors on the battlefield as an intelligent minefield to detect and monitor enemy movement. The sensors can be spread out using aeroplanes or submunitions. An interesting civilian usage of these "intelligent minefields" can be found in accidents and catastrophe sites such as after an earthquake where humans can be trapped and wounded and need to be found quickly [4].

The usage for the WSN we are proposing is entirely related to traffic. One interesting application can be seen in Figure 3.1 and is a queue warning system. The sensor nodes collaborate and send a signal to the warning unit if there is a queue.

3.2 Wireless Hardware

The transceiver could use IEEE 802.15.4 and ZigBee[1] standards [5]. The exact design of the WSN is not decided upon, here ZigBee is used for simplicity. The sensor nodes should be able to perform short-range communication in small networks for which ZigBee and Wireless Personal Area Networks (WPANs) are ideal. Unlike Wireless Local Area Network (WLANs), WPANs allow for small, power-efficient, inexpensive solutions for a wide range of devices since they do not involve any or very little infrastructure [6].

3.2.1 ZigBee Networks

A Low-Rate Wireless Personal Area Network (LR-WPAN) is a simple, low-cost communication for applications where resources are limited [6]. An LR-WPAN offer easy installation, reliable communication, short-range operation, low cost and low power consumption. Two types of devices can exist in such a network; reduced-function devices (RFD) and full function-devices (FFD). A FFD can talk to everyone while an RFD can only talk to a FFD. ZigBee Alliance defines the network, security and application support layers (API) on top of the physical (PHY) and media access layer (MAC) defined by IEEE Standard 802.15.4 [6, 7].

The network will consist mostly of sensor nodes (SNs) which are RFDs. These can unlike the FFDs, not become the coordinator in the star topology net used in this implementation [6, 7]. We will use an access point (AP) to transmit data to the backbone network. The network topology can be seen in Figure 3.2. In the future, we will like to have the option to use a mesh network topology instead. This will allow us to use SNs as relays.

3.3 Wireless Sensor Networks for applications related to traffic

Due to the different applications, the requirements for a WSN are also different. In our application some of the important requirements are

- **Multihop (wireless) communication.** Sending information over large distances is only

[1] ZigBee Alliance, `www.zigbee.org`

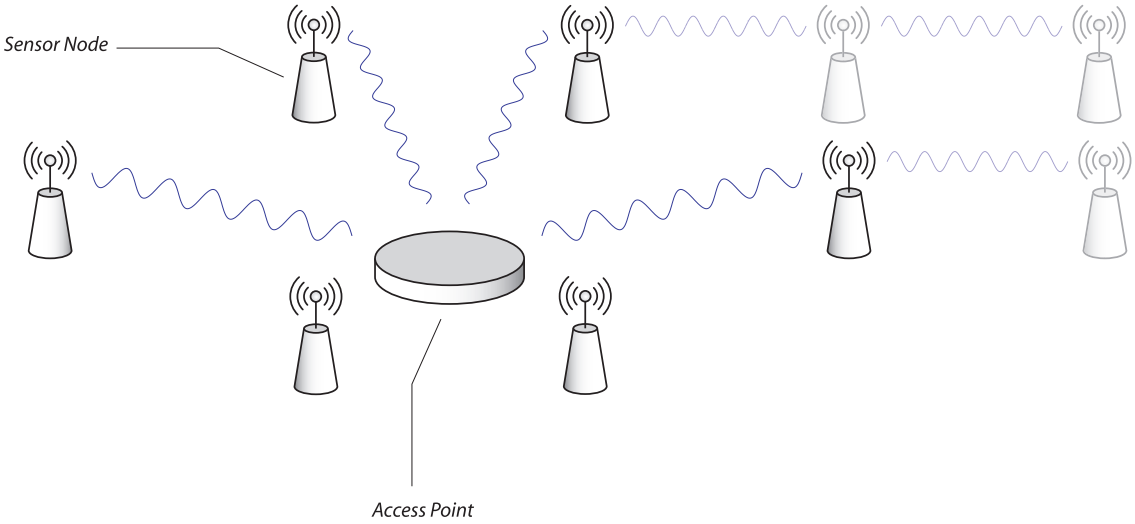

Figure 3.2: *Star network topology with network coordinator [6, 7]. The network coordinator is in our application the access point (AP) and the nodes are the wireless sensor nodes (SNs).*

possible using high transmission power. By using sensor nodes as relays we can reduce the required power.

- **Energy-efficient operation.** Since the nodes are battery powered a strict power consumption policy is needed. When parts of the sensor node are not needed they are put to sleep only to be awaken when they are needed.

- **Auto-configuration.** The nodes should be easily installed, by anyone, anywhere and at any time. If the sensor nodes, and the wireless network, can be auto-configured it would be hugely beneficial. A "must-have" property [8] of the sensor nodes is that they should autonomously position themselves in the network. Preferably they should not rely on surrounding infrastructure such as the Global Positioning System (GPS). There are many different techniques that forms the basis for autonomous positioning.

- **In-network processing.** An individual node may not be able to determine whether an event has occurred or not but will depend on collaboration with its neighbours. We would like to keep the inter-node traffic as low as possible to keep the power consumption low at the same time as any calculations will take time, memory and power.

The amount of processing needed in the SNs is highly dependant on their use. There are three main usages for our equipment

- **Vehicle detection, speed estimation and counting,**

- **Vehicle classification,**

- **Queue detection. See Figure 3.1.**

There is also a possibility to re-identify vehicles [9]. This requires more SNs and more computational power.

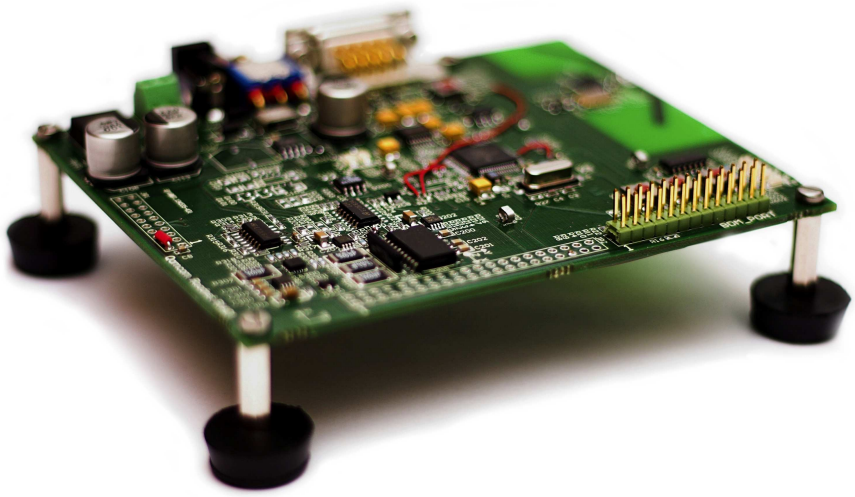

Figure 3.3: *Wireless Sensor Node Prototype.*

3.4 Sensor Node Hardware

The sensor node is comprised of two main parts, seen in Figure 3.4. The primary intent of the sensor node is obviously to sense something and therefore the sensor or sensors make up one of those parts. Our sensor node uses magnetoresistive sensors to sense the magnetic field and it is sensitive enough to detect field in the range of at least tens of nanotesla. The prototype can be seen in Figure 3.3. In order to understand why we have chosen anisotropic magnetoresistors we have to look at the arguments for and against other systems.

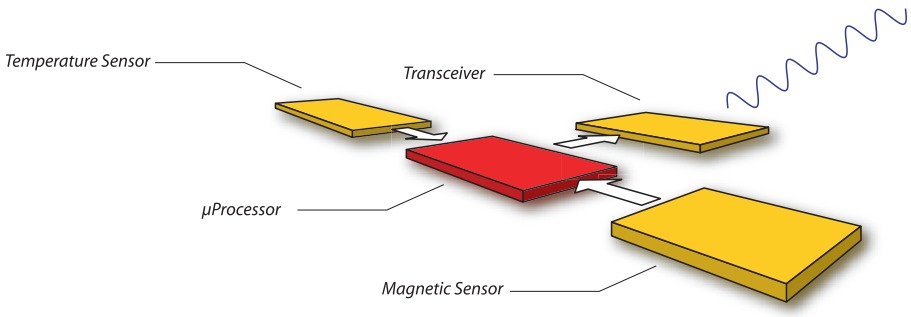

Figure 3.4: *Wireless Sensor Node Architecture.*

3.4.1 Comparison of existing technologies

The different surveillance technologies can be classified as intrusive, non-intrusive or off-roadway [10]. Intrusive sensor systems are installed in or on the pavement, non-intrusive are installed over or at the side of the road. Off-roadway systems are special since they need no equipment installed on-site.

Inductive loop

The energy is used for measuring change in oscillator frequency [10] over the sensor loop and for analog to digital (A/D) conversion [11]. The inductive loop is therefore an active sensor. Inductive loops are today the most common vehicle detector in use and is today a mature technology. It has a high detection accuracy. The disadvantages include high-cost installation and traffic disruption during installation. The loop wire is affected by stresses in the road surface and temperature making the failure rate high [10].

Pneumatic Tube

A pneumatic tube system is a very basic system that uses pressurised tubes to measure traffic parameters. When a vehicle passes the tube a pulse of air pressure is transferred along the tube. The output is therefore only detection, however with more than one tube, you can find the speed and even classify vehicles. The simplicity of this system is apparent. One of the major drawbacks, especially in Sweden, is that measurements can not be done in the winter time due to the possibility that the tubes will be plowed away by snow plows.

Installation and maintenance costs are kept low due to its simplicity. Drawbacks include inaccuracy in axle counting when buses and trucks are common [10]. The sensitivity is temperature dependant, and the equipment wear and tear is significant.

Piezoelectric sensor

A piezoelectric sensor uses a material that will generate an electrical potential when mechanical stress is applied. The output is proportional to the force applied and is only present when the force is changing. Classification is done here by axle count, spacing and vehicle weight. These types of sensors also have high-cost installation and maintenance.

Weigh-In-Motion system

A Weigh-In Motion (WIM) system will estimate the gross weight of a passing vehicle using different types of technology embedded in the road or on the road. These sensors can be of the piezoelectric type described previously. They can also depend on a capacitance mat, on hydraulic fluid in a pressure transducer (load cell sensor) or fiberoptics. A fiberoptic system is popular since it is installed by sticking thin tubes onto the pavement as opposed to burying the sensors [10].

Infrared-based system

An infrared-based system can be either passive or active. A passive system relies on the emitted radiation from vehicles and ground surfaces while an active system uses the time difference between transmit and receive of the reflected pulse. The performance of the system is greatly affected by the environment, for example rain and snow, sunlight and temperature.

Ultrasonic system

Ultrasonic sound waves are used for ranging in these systems and the principle is similar to that of a radar. There are models using Doppler shift to measure speed. Disadvantages include temperature and wind dependence [10].

Passive acoustic system

By using an array of microphones, the acoustic energy produced by a vehicle is measured. Performance is affected by temperature and accuracy drops with slow moving vehicles [10].

Video Image Processing

A video traffic detection system relies on image processing of optical data and therefore it is affected by weather conditions and lighting conditions. The system can also be affected by traffic intensity, and camera placements since vehicles in the background will make it harder for the image processing algorithms.

Microwave Radar

A radar system works in the same way as a video system but since it is not using optical wavelengths it is not affected by weather and lighting conditions to the same degree. It is however affected by traffic intensity and radar sensor placement. There are a number of different types of radar systems, each with its advantages and disadvantages. A continuous wave (CW) radar estimate the vehicle speed with the use of a single radar sensor. With the use of frequency-modulated continuous wave (FMCW) radar, a pair of of radar zones must be used.

Off-roadway technologies

These systems do not need any roadside hardware. Technologies include Global Positioning System (GPS) positioning of mobile phones and Automatic Vehicle Identification (AVI). Positioning by mobile phones is interesting because it is rare that any vehicle do not have a mobile phone so no equipment need to be installed. Remote sensing by satellite or aircraft, optical or radar, can be used but has limited coverage due to the low availability of aircraft and satellites.

3.4.2 Summary of different technologies

In Tables 3.1 and 3.2 a comparison between the different technologies are presented. In Table 3.1 we can see the capabilities of the different systems and in Table 3.2 we can find what affects their performance. There is of course a big difference in installation cost and maintenance costs for these systems and the data they produce differ in accuracy. Inductive loops, which are the most used today, have a very good accuracy but are expensive. A WSN also has a good accuracy but is much cheaper, and can outperform the inductive loop. There are also differences within the same system. For example a side-fire or overhead-fire VIP system has much different performance.

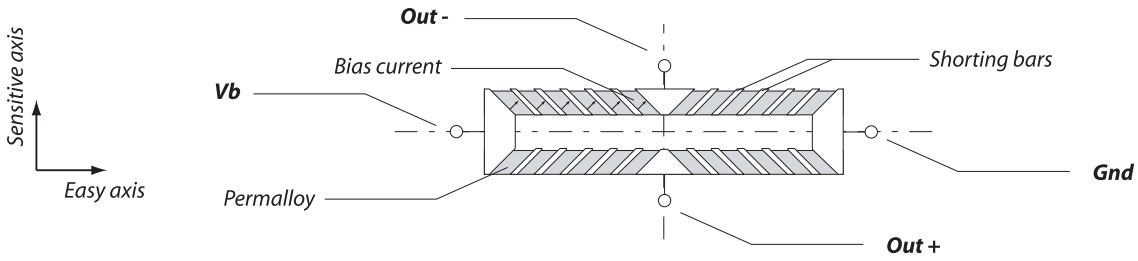

Figure 3.5: *AMR Barber Pole Bias.*

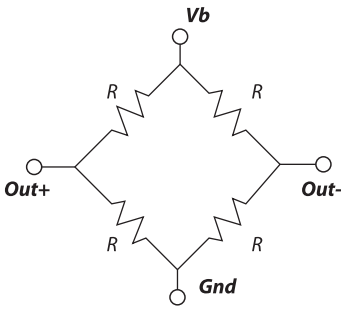

Figure 3.6: *Wheatstone bridge. Voltage difference between* OUT+ *and* OUT- *is measured.*

3.4.3 AMR Magnetic sensors

Some materials change their electrical resistance when exposed to a magnetic field [12]. This magnetoresistive effect is used in anisotropic magnetoresistance sensors (AMR) sensors. The resistive elements are most often made of nickel-iron [13] (Permalloy) thin films.

The benefits of using this type of sensor come from its ability to sense static magnetic fields as well as the direction of those fields. The detection range is also suitable for our purposes. They are very sensitive to magnetic fields – according to [12] they have a noise specification of in the order of $\mathrm{nT}/\sqrt{\mathrm{Hz}}$ and one of the sensors we are using has a resolution of 2.7 nT. As a comparison computer floppy disks store data with field strengths of approximately $1 \cdot 10^6$ nT [14]. Another important fact is that the sensors can be bulk manufactured on silicon wafers, and thus are cheaper.

In an AMR sensor these magnetorestive materials are used in a "Wheatstone bridge" [15]. A typical AMR sensor bridge can be seen in Figure 3.5 and the electrical diagram of a Wheatstone bridge can be seen in Figure 3.6. Each bridge has four resistive elements which are ordered so that opposite elements are equal. If a magnetic field is applied, two of the resistive elements will decrease slightly in resistance. The other two will increase slightly.

The voltage between the out terminals Out_+ and Out_- on the sensor is measured. That voltage is dependant on the sensor sensitivity, the bridge supply voltage and the applied field [15].

$$\mathrm{Out}_+ - \mathrm{Out}_- = SV_bB_s, \tag{3.1}$$

where S is the sensor sensitivity [mv/V/T], V_b the bridge supply voltage and B_s the applied

magnetic field [T]. In order to detect a magnetic field of any orientation we will need three of these sensors – one for each axis.

The properties of the AMR sensor are only well-behaving when the magnetic domains of the film is aligned with each other. The "easy axis" of the magnetisation vector $\boldsymbol{M}$ is set during fabrication, see Figure 3.7a. The $\boldsymbol{M}$ vector is then parallel to the length of the resistor. The low-resistance shorting bars (seen in Figure 3.5) is there to make the current flow at a 45 degree angle to the film which gives us an angle θ between the current vector and the magnetisation vector. The resistance is dependent on the angle θ and reaches its maximum when the current vector is parallel to the magnetisation vector [13]. The technique for producing this "shortest path" through the resistor is called barber pole biasing.

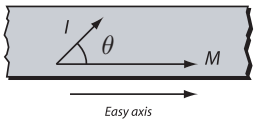

Figure 3.7a: *Magnetoresistive effect. Permalloy (NiFe) resistor [13], no applied field.*

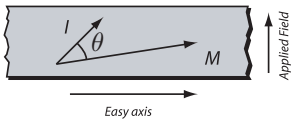

Figure 3.7b: *Magnetoresistive effect. Permalloy resistor, applied field.*

If we now apply a magnetic field normal to the easy axis the magnetisation vector will rotate and we will see a change in the voltage output of the Wheatstone bridge. The magnetoresistive effect is directly related to the angle θ [16]. See Figure 3.7b.

A magnetic field will break down the alignment of the magnetisation vector which is essential to receive accurate measurements. The resistor is made up of many magnetic domains whose magnetisation vector can point in any direction, see Figure 3.8a. For small disturbances, these magnetic domain magnetisation vectors will rotate back to their previous direction when the field is no longer applied. For large fields however they will not. To realign the total magnetisation vector with the easy axis we can apply a strong magnetic field in the right direction. The Honeywell sensors are for this reason equipped with a Set/Reset (S/R) strap that can be pulsed with high current to reset the sensor and align the magnetisation vector with the easy axis again. The effect of the S/R pulses can be seen in Figure 3.8b and 3.8c.

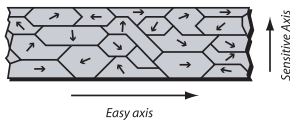

Figure 3.8a: *Random magnetic domain orientations [16, 17] before set/reset pulse. Note the sensitive axis.*

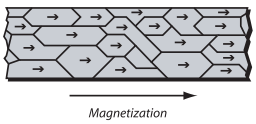

Figure 3.8b: *Magnetic moment domain orientations after a set pulse [16, 17]. Moments aligned to the right.*

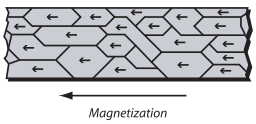

Figure 3.8c: *Magnetic moment domain orientations after a reset pulse [16, 17]. Moments aligned to the left.*

We need to create the current through the S/R strap and this is done using an H-bridge. The current pulse shape can be seen in Figure 3.9. The S/R current has a high power requirement. We need to minimise the current, and maximise the time between the S/R pulses in order to conserve battery power. A number of schemes for doing this has been tested, among those are

- Use only set or reset pulse at any time, interchange them,
- Use less current for each pulse,
- Maximise the time between pulses,

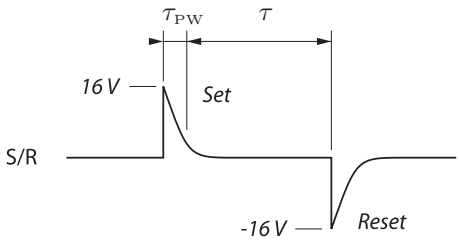

Figure 3.9: *Set/Reset pulses of HMC100x, HMC1043.*

- Only S/R when a high field has been present.

It is most likely that a combination of the above will produce the best result. An important parameter in this is the usage of the sensor. If we need to detect small fields, then we need to do this more often.

3.5 Sensor Hardware

The sensor nodes should be inexpensive, battery powered (maybe with an option for an external power source), rugged, easy to maintain, and easy to install. A prototype sensor node has been built by a previous project [5] at Qamcom Technology AB.

The sensor should be easy to operate, be capable of near-real-time calculations and withstand road conditions in the most demanding of climates. Here in Sweden the climate offer snow and ice in the winter and high temperatures in the summer. It should be able to operate for a long time in these climates putting enormous strain on the power supply. The power supply can be internally or parasitically powered.

Table 3.1: *Capabilities of different technologies [10].*

Technology	Presence	Count	Direction	Speed	Classification
Pneumatic tube		•	•	•	Wheel axes
Piezoelectric sensor		•	•	•	Wheel axes
WIM system	•	•	•	•	Wheel axes
CW radar		•	•	•	
FMCW radar	•	•	•	•	Shape
Active infrared	•	•	•	•	Shape
Passive infrared	•	•	•	•	Shape
Video Image Processing	•	•	•	•	Shape
Ultrasonic	•	•	•	•	Shape
Passive Acoustic	•	•	•	•	Sound
Inductive loop	•	•	•	•	Magnetic signature
AMR Sensors	•	•	•	•	Magnetic signature

Table 3.2: *Sensitivity of technologies to environmental effects [10].*

Technology	Wind	Temperature	Lighting	Traffic flow
Inductive loop		•		
Pneumatic tube		•		•
Piezoelectric sensor		•		
WIM system				
CW radar				•
FMCW radar				
Active infrared				
Passive infrared				
Video Image Processing		•	•	
Ultrasonic	•			
Passive Acoustic	•	•		•
AMR Sensors		•		

Chapter 4

Theoretical model

This is were we come to the pith of the matter. A vehicle is made up of different magnetic materials. Some of them are soft magnetic materials and some are hard magnetic materials [12]. The soft magnetic materials have no residual magnetisation but high magnetic susceptibility. The hard magnetic materials have high residual magnetisation. These materials all have the property that they will disturb a present magnetic field. The disturbances in a magnetic field created by a vehicle are large enough to be detected with a magnetic sensor.

Different vehicles will disturb a magnetic field differently due to the different magnetic materials and their distribution within the vehicle.

4.1 The earth magnetic field

The magnetic field that we live and work in everyday is always changing. For this application it is of critical importance that the earth magnetic field does not change too rapidly, at least not during the passing of a vehicle.

The magnetic field in a particular position has been known to be affected by magnetic mineral, iron artifacts, and similar. Short-term effects from solar flares are frequent. The earth magnetic field reverses polarity with an estimated frequency of a quarter of a million years. On a more rapid time scale, the field is estimated to have decayed about 5–15 % over 150 years [18]. Even if the decay is twice as much, it would not pose a problem for our application.

The earth magnetic field looks very different depending on your location in the world. The measurements discussed in this thesis have all been made in Göteborg, Sweden[1]. A common and non-complex model of the earth magnetic field can be seen in Figure 4.1.

[1] Lat 57 43 00 N Long 011 58 00 E

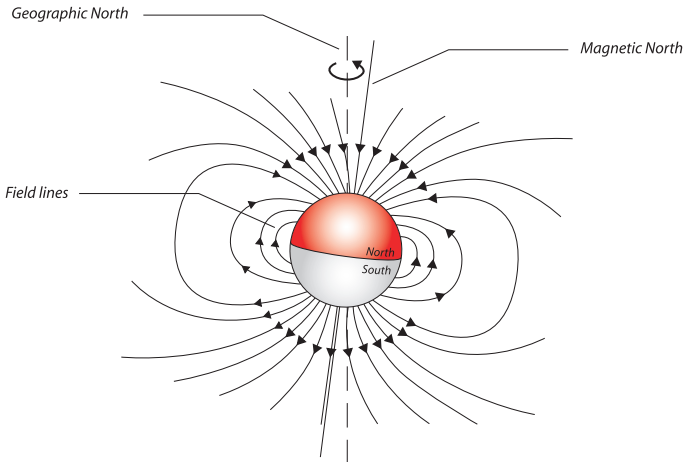

Figure 4.1: *Simplified model of the earth magnetic field. The earth magnetic field can be modelled like an ordinary magnet but in reality it is much more complex and is changing constantly.*

4.2 Sensing the world

The primary intent of a magnetic sensor is often not measuring the magnetic field. Instead one wishes to measure other parameters such as speed, heading, and presence, and to do so one has to look at the effect those parameters have on the magnetic field. Figures 4.2a and 4.2b illustrates the difference between conventional sensing and magnetic sensing. In order to get the parameters we want from the magnetic fields, we have to apply signal processing.

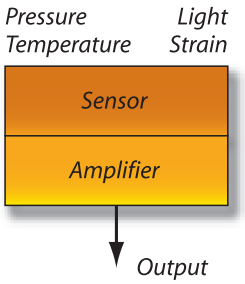

Figure 4.2a: *Conventional sensing.*

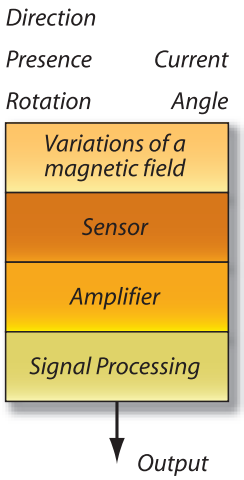

Figure 4.2b: *Magnetic sensing.*

4.3 Magnetic model

When a vehicle moves into a magnetic field the magnetic field lines are disturbed. These disturbances are not located solely inside the vehicle but also outside, allowing us to measure the magnetic field in order to sense the presence of that vehicle. See Figures 4.3a and 4.3b.

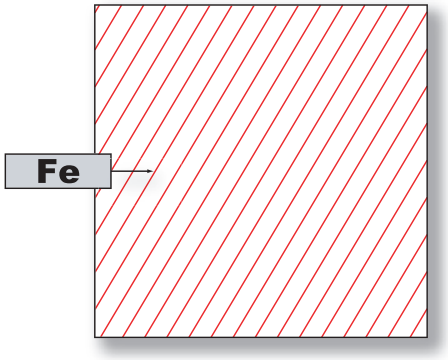

Figure 4.3a: *Non-disturbed field lines. A vehicle is about to enter.*

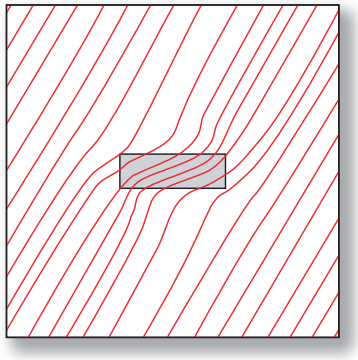

Figure 4.3b: *Field lines distributed by a passing vehicle. Simulated in* FEMLAB[2].

All electromagnetics are governed by Maxwell's equations [19–21],

$$\nabla \cdot \boldsymbol{D} = \rho_c \qquad \text{Gauss's law} \tag{4.1}$$

$$\nabla \cdot \boldsymbol{B} = 0 \qquad \text{Gauss' law for magnetism} \tag{4.2}$$

$$\nabla \times \boldsymbol{E} = -\frac{\partial \boldsymbol{B}}{\partial t} \qquad \text{Faraday's law of induction} \tag{4.3}$$

$$\nabla \times \boldsymbol{H} = \boldsymbol{J} + \frac{\partial \boldsymbol{D}}{\partial t} \qquad \text{Ampère's circuital law (with Maxwell's correction),} \tag{4.4}$$

where $\boldsymbol{B}$ is the magnetic flux density, $\boldsymbol{H}$ is the magnetic field strength, $\boldsymbol{E}$ is the electric flux density, $\boldsymbol{D}$ is the displacement field, $\boldsymbol{J}$ is the current density and $\mu_0 = 4\pi \cdot 10^{-7}$ Vs/Am is the permeability in vacuum [21]. μ_r is the relative permeability of the medium and ρ_c is the electric charge density. In linear materials

$$\boldsymbol{D} = \varepsilon_0 \boldsymbol{E} + \boldsymbol{P} = (1 + \chi_e)\varepsilon_0 \boldsymbol{E} = \varepsilon \boldsymbol{E}, \tag{4.5}$$

$$\boldsymbol{B} = \mu_0(\boldsymbol{H} + \boldsymbol{M}) = (1 + \chi_m)\mu_0 \boldsymbol{H} = \mu_0 \mu_r \boldsymbol{H}, \tag{4.6}$$

where $\boldsymbol{P}$ is the polarisation density, $\boldsymbol{M}$ is the magnetisation density, χ_e is the electrical susceptibility and χ_m is the magnetic susceptibility. Assuming that the magnetic field is changing slowly, so that we reach a steady state, Maxwell's equations reduce [19–21] to the magnetostatic equations

$$\nabla \cdot \boldsymbol{B} = 0 \qquad \text{Gauss' law for magnetism} \tag{4.7}$$

$$\nabla \times \boldsymbol{B} = \mu_0 \mu_r \boldsymbol{J} \qquad \text{Ampère's circuital law.} \tag{4.8}$$

The vector potential of a magnetic dipole [20, 21] can be written as

$$\boldsymbol{A}(\boldsymbol{\mu}, \boldsymbol{r}) = \frac{\mu_0}{4\pi} \frac{\boldsymbol{\mu} \times \boldsymbol{r}}{|\boldsymbol{r}|^3}, \tag{4.9}$$

where $\boldsymbol{\mu}$ is the magnetic moment and $\boldsymbol{r}$ is the vector from the dipole. This can be related to the magnetic flux density [21] by

$$\boldsymbol{B} = \nabla \times \boldsymbol{A}. \tag{4.10}$$

The field from a magnetic dipole moment [22] situated at the origin can then be written in vector form as

$$\boldsymbol{B}(\boldsymbol{\mu}_i, \boldsymbol{r}_i) = \frac{\mu_0}{4\pi} \frac{3\,(\boldsymbol{\mu}_i \cdot \boldsymbol{r}_i)\,\boldsymbol{r}_i - \boldsymbol{\mu}_i\,|\boldsymbol{r}_i|^2}{|\boldsymbol{r}_i|^5}, \quad \boldsymbol{r}_i, \boldsymbol{\mu}_i \in \mathbb{R}^3. \tag{4.11}$$

[2]Now COMSOL MULTIPHYSICS, `http://www.comsol.com/`

Table 4.1: *Maximum magnetic field strength at different distances from a passing passenger car. The node is placed in the road surface.*

Distance [m]	$\lvert B_z \rvert$ [nT]
0	$2.2 \cdot 10^5$
1	1765
2	322
3	102

Table 4.2: *Maximum magnetic field strength at different distances from a passing passenger car. The node is placed at a height of 0.3 m.*

Distance [m]	$\lvert B_z \rvert$ [nT]
0	$2.5 \cdot 10^{11}$
1	3000
2	375
3	111

The total magnetic field, $\boldsymbol{B}$, from n individual magnetic moments [22] can be written as

$$\boldsymbol{B}(\boldsymbol{r}_1, \boldsymbol{\mu}_1, \boldsymbol{r}_2, \boldsymbol{\mu}_2, ..., \boldsymbol{r}_n, \boldsymbol{\mu}_n) = \frac{\mu_0}{4\pi} \sum_{i=1}^{n} \frac{3\left(\boldsymbol{\mu}_i \cdot \boldsymbol{r}_i\right)\boldsymbol{r}_i - \boldsymbol{\mu}_i \left|\boldsymbol{r}_i\right|^2}{\left|\boldsymbol{r}_i\right|^5}, \tag{4.12}$$

where $\boldsymbol{r}_i$ is the position for the ith magnetic moment $\boldsymbol{\mu}_i$.

It is assumed in [22] that the permanent and induced magnetic fields from a vehicle can be viewed as the field from a number of magnetic moments. We shall later see that this is a good assumption. If we have knowledge of all the positions and strengths of the magnetic moments within the vehicle, we can calculate the field from that vehicle in any point in space. However, we will have an infinite number of magnetic moments.

Each of the magnetic moments will have six degrees of freedom, making a large system very complex to handle. Each vehicle will therefore be approximated to be comprised of a low number of magnetic moments.

The earth magnetic field will have different direction and strength at different locations, but we can assume it to be constant near the sensor so that a vehicle will experience the same field in the vicinity of the sensor node. We also assume that the field does not change during the vehicle's passing of the sensor. The earth magnetic field does not have to be exactly equal at two different sensor node positions since the disturbances caused by the vehicle is similar. They are however not the same due to the orientation of the earth magnetic field and its impact on the magnetic dipole moments we assume our vehicle to be comprised of. For this application we assume that the magnetic dipoles are not time dependant. The time dependant magnetic field can now be written as

$$\boldsymbol{B}(\boldsymbol{r}_1(t), \boldsymbol{\mu}_1, \boldsymbol{r}_2(t), \boldsymbol{\mu}_2, ..., \boldsymbol{r}_n(t), \boldsymbol{\mu}_n) = \frac{\mu_0}{4\pi} \sum_{i=1}^{n} \frac{3\left(\boldsymbol{\mu}_i \cdot \boldsymbol{r}_i(t)\right)\boldsymbol{r}_i(t) - \boldsymbol{\mu}_i \left|\boldsymbol{r}_i(t)\right|^2}{\left|\boldsymbol{r}_i(t)\right|^5}. \tag{4.13}$$

4.4 Vehicle model

In the model used, a vehicle of any type is said to be equivalent to at most three magnetic moments distributed in the car seen in Figure 4.5. A few simplifications are hereby made. The moments are assumed to be placed on the centerline of the vehicle, thereby reducing the degrees of freedom per magnetic moment by two. Since we have three magnetic moments each now having four degrees of freedom, we have a total number of twelve degrees of freedom. Compare this to the eighteen we had originally or even the unlimited degrees of freedom we really have. This is certainly a limitation of the model. The vehicle will move in a coordinate system relative to the sensor, where the sensor is placed in the origin.

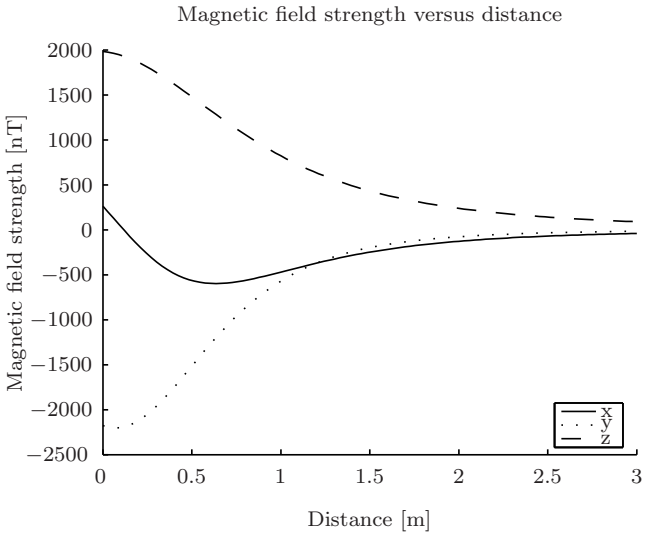

Figure 4.4: *Magnetic field strength depending on distance. The sensor is placed on the road surface and the field is measured exactly when the vehicle passes the sensor. This is not the point where the field is the strongest.*

The simulated maximum sfield strengths from a single passenger vehicle pass versus distance to sensor can be seen in Tables 4.1 and 4.2 The simulated maximum field strengths versus distance at the instant the vehicle passes the sensor can be seen in Figure 4.4.

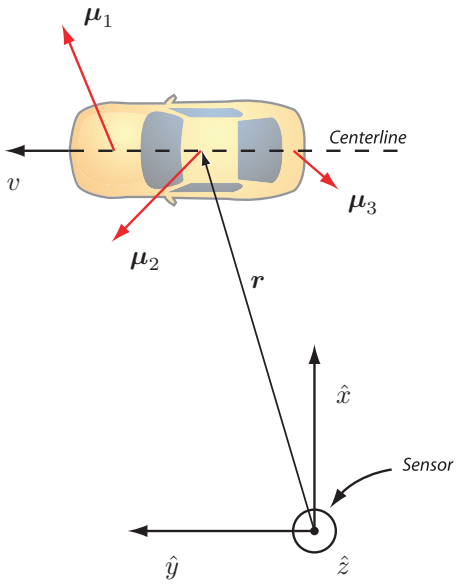

Figure 4.5: *Input parameters to the* MATLAB*-model. The sensor is placed at the origin. The magnetic dipoles are assumed to be positioned on the vehicle centerline.*

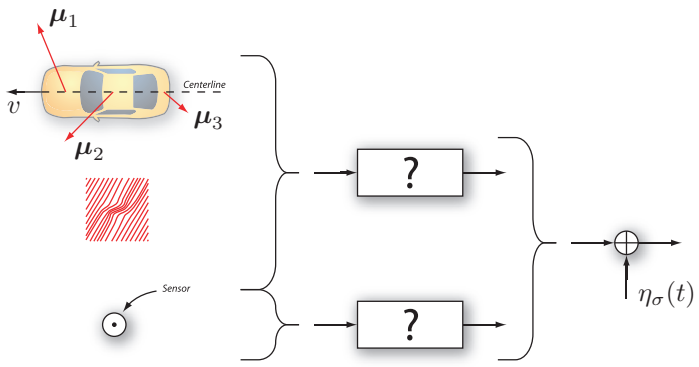

Figure 4.6: *Can our channel be modelled as an AWGN channel?*

4.5 Sensor and channel model

It is assumed that the data is affected by additive white Gaussian noise with some power as can be seen in Figure 4.6. We do not know exactly what the channel will do to the magnetic field, and we do not know exactly what the sensor will introduce, but their joint effect is modelled as an Additive White Gaussian Noise, AWGN, channel. The signal in one of the sensor axis is then represented by

$$x_i(\boldsymbol{r}_1(t), \boldsymbol{\mu}_1, \boldsymbol{r}_2(t), \boldsymbol{\mu}_2, ..., \boldsymbol{r}_n(t), \boldsymbol{\mu}_n) = B_i(\boldsymbol{r}_1(t), \boldsymbol{\mu}_1, \boldsymbol{r}_2(t), \boldsymbol{\mu}_2, ..., \boldsymbol{r}_n(t), \boldsymbol{\mu}_n) + \eta_{i,\sigma}(t), \quad (4.14)$$

where $\eta_{i,\sigma}(t)$ is a zero-mean Gaussian distributed random variable with standard deviation σ in direction $i \in \{\hat{x}, \hat{y}, \hat{z}\}$.

4.5.1 Reconstruction

As will be shown later we have sampled the signal at more than twice the Nyquist frequency and our signal $x(t)$ with one-sided baseband bandwidth W is therefore uniquely determined by its samples

$$x[n] = x(nT_s) \quad n = 0, \pm 1, \ldots \quad (4.15)$$

if the sampling frequency is

$$f_s = \frac{1}{T_s} > 2W \quad (4.16)$$

where the Fourier transform $X(f)$ of $x(t)$ satisfies

$$X(f) = 0 \quad |f| > W. \quad (4.17)$$

$2W$ is called the Nyquist rate, and $f_s/2$ is the Nyquist frequency. We can now reconstruct the signal $x(t)$ by lowpass filtering [23] the train of impulses $x(nT_s)\delta(t - nT_s)$. This will give us the reconstruction as

$$x(t) = \sum_{n=-\infty}^{\infty} x(nT_s) \frac{\sin(\pi(t - nT_s)/T_s)}{\pi(t - nT_s)/T_s}. \quad (4.18)$$

4.6 Comparison to real world data

Simulated data from four different vehicles can be seen in Figures 4.7a through 4.7d. The sensor has been placed 1.5 m from the vehicles on the left side on the road surface. The speed was 100 km/h. No noise was added. For the passenger car, one dipole situated 0.3 m over the sensor in the $\hat{z}$-direction and 0.7 m from the sensor in the $\hat{x}$-direction. The magnetic dipole strength was $[-3, 0, -30]\,\mathrm{Am}^2$, i.e., almost entirely in the negative $\hat{z}$-direction as expected at this location.

A comparison between simulated and real data for all axes can be found in Figures 4.8a and 4.8b. There are some discrepancies due to the fact that there are many unknown parameters in the measured data, such as velocity and distance to the sensor and these had to be estimated before simulation.

From this simple comparison we can conclude that our model is a reasonable model. However, we can not say anything about how good it is from this case where numerous parameters are unknown.

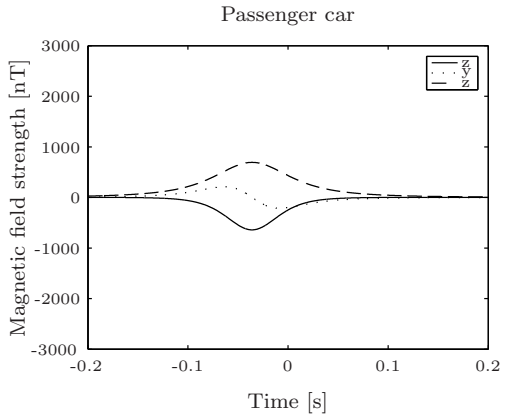

Figure 4.7a: *Simulated sensor data from passenger car.*

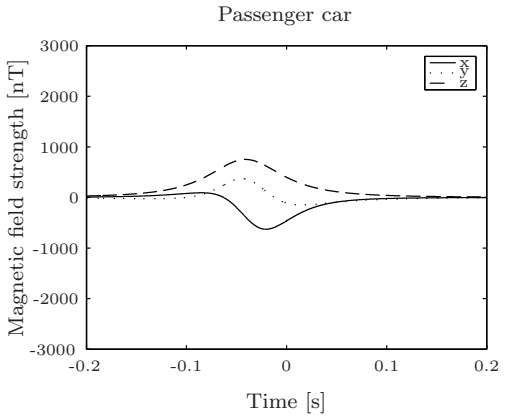

Figure 4.7b: *Simulated sensor data from another passenger car.*

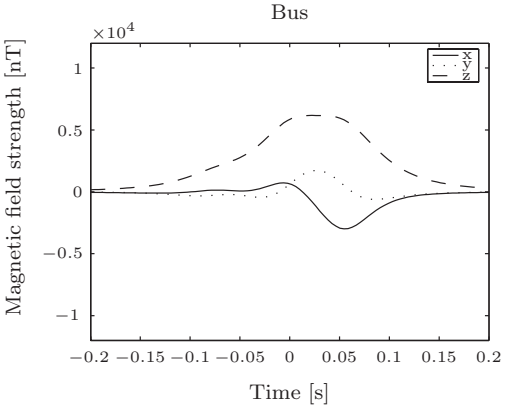

Figure 4.7c: *Simulated sensor data from bus. Note the complexity.*

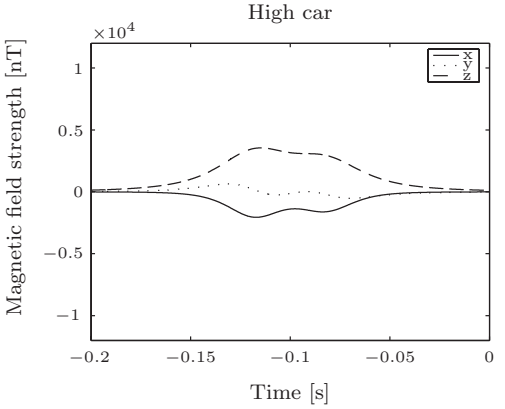

Figure 4.7d: *Simulated sensor data from high car. Note the complexity.*

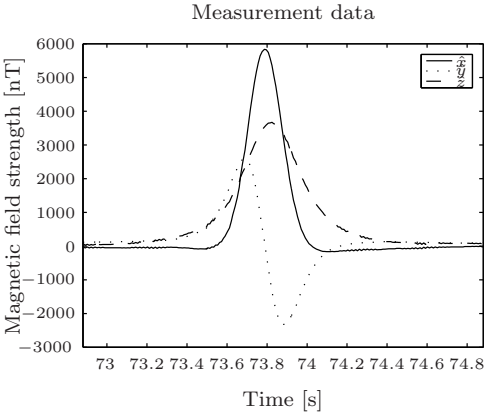

Figure 4.8a: *Measured sensor data from passenger car [22]. Note the different timescale due to difference in speed.*

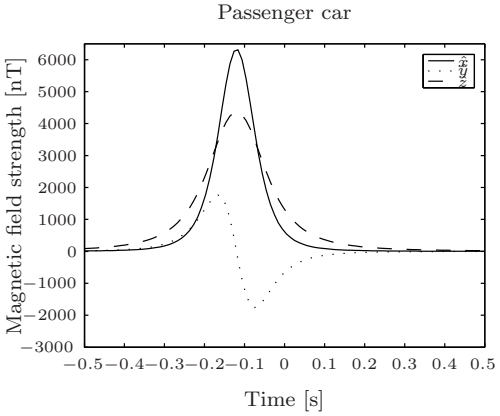

Figure 4.8b: *Simulated sensor data from passenger car. Speed was 30 km/h and the distance to the sensor was 0.7 m. The sensor was placed on the roadway.*

Chapter 5

Algorithms

5.1 System Overview

This chapter will describe the algorithms that could be used in our system. For each node we have the option to put the sensor node in the center of the lane, at the side of the lane or anywhere in between. The first two positions will give rise to much different characteristics in the signal so the position will be important when assessing the algorithms. An overview of the system can be seen in Figure 5.1.

5.2 Simulation of traffic

It is more important to monitor oversized vehicles such as buses and trucks than other types of vehicles. These vehicles have distinctively different characteristics in terms of speed, acceleration, road space, and manoeuvre times [24]. They also have longer breaking times and are sometimes only permitted to drive in certain lanes or even roads. The heavier vehicles will contribute disproportionally to the wear and tear of the road surface. In this thesis, the focus has however been laid on passenger cars, buses and high cars or SUVs. Together they give rise to very different types of sensor outputs and can be used for most simulation purposes. Since these types are the most common we can feel confident that our algorithms will work. The model takes into account the different probabilities of the different vehicle types, and more types of vehicles can be added.

A traffic model can be very complex. In this thesis it is assumed that all vehicles travel along the same line, at the same velocity. Furthermore, they do not accelerate, the vehicle path is parallel to the sensor $\hat{y}$-axis and they all have the same height. In the simulator it is easy to implement another traffic model if needed.

5.3 Detection

We need to have enough samples in order to distinguish key features in the vehicle. The number of samples needed is of course determined by the application. If we wish to merely detect a vehicle,

we need at least one sample when the vehicle is passing the sensor and generate a signal with an amplitude over a pre-defined threshold value. If we assume that no vehicle will travel faster than 110 km/h, we will need to sample at 7 Hz in order to get one sample at a time where a part of the vehicle is directly above the sensor. However, it is not certain that every part of the vehicle will generate a signal greater than the threshold value. It is not even guaranteed that the maximum will occur exactly when the vehicle passes the sensor. If we instead need to *classify* vehicles, we will need many more samples. If we need four times more samples, the highest frequency will be less than 40 Hz. Since we need to sample faster the twice the Nyquist frequency we find that a sampling frequency of 100 Hz is enough, and this hypothesis is strengthened by the FFT of simulated and measured data. In the literature a sampling frequency from 64 Hz to 128 Hz is reported [11]. The sampling frequency is in some cases up to 2 kHz [25] for short periods of time, which is thus unnecessary. We would like to keep the sampling frequency to a minimum – if we sample less often we can let the sensor and processor sleep longer to reduce power consumption.

5.3.1 Thresholding

Detection using simple threshold values is not as simple as it might sound to the casual reader. The sensor output is temperature dependant and the effect will be significant. However the temperature change can be made slow in comparison to the magnetic signature of a vehicle by clever design of the enclosure. An illustration of the temperature dependant offset can be seen in Figure 5.2.

The threshold value can be set at design time or by training the sensor. An adaptive algorithm can be used to make sure that the threshold is larger than the noise and change depending on temperature. The threshold value also depends on the closeness to disturbing traffic etc.

5.3.2 Target Tracking

If we have many small sensor nodes with only one task – to report the magnetic equivalent to Received Signal Strength Indication (RSSI) values – we can track vehicles within the area covered by the WSN. This is a known problem, commonly encountered in radar systems. In our case we will have different sensor nodes i.e. a spatial problem and in a radar system you will have different directions at different times, i.e. a time dependant problem. We have decided not to give this area any focus even though target tracking will be implementable in our system if sensors are positioned for such an application.

5.4 Direction

Direction can be found by a single sensor node [15]. The sensor should be placed at the side of the road, and the $\hat{\boldsymbol{y}}$-axis response will show the direction of travel. The signature for a vehicle travelling in the forward direction can be seen in Figure 5.3 – a vehicle travelling in the reverse direction will produce a mirrored signature. Note that the sensor placement and the dipole orientation will affect the signature.

However a more reliable method involves using two sensor nodes, a SN pair, to find the speed and thereby the direction. In order for this to work the SN pair needs to be time synchronised in order for this to work and the distance between them must be known.

5.5 Speed estimation

Speed estimation can be either one of two things – the estimation of the speed of an individual vehicle or the average speed of a number of vehicles in an area. The algorithms used for these estimations use different parameters that can be seen in Figure 5.4 and the definitions can be found in Chapter 2. We can use a single sensor, or more sensors, to find a speed estimation.

To find the speed in the two-sensor case we need to consider the distance between the sensors. A large distance between the sensors means that we will not need a high sampling rate. The sampling rate needs to be large compared to the velocity. The velocity in turn depends on the time and the distance between sensor nodes which means that the inverse sampling rate, the sampling period, should be small compared to the time it takes for a vehicle to pass the SN pair.

A large distance will also mean that we will get a average velocity as opposed to a instantaneous velocity, a shorter distance will get us closer to the instantaneous velocity. However, the error in velocity due to error in time difference will decrease when the distance is increased. Since it is difficult to synchronise clocks between sensors, it will however be beneficial to put two sensors in the same node but placed at a distance from each other on the circuit board. In this case we can let the second sensor sleep until the first sensor triggers and then start to sample both sensors at a higher rate in order to minimise the error. The fact that we can let one sensor sleep lets us save power and money since we do not need a dedicated processor and transceiver for the extra sensor.

5.5.1 Speed of an individual vehicle

Traditional time difference

Using two sensors we can estimate the speed for an individual vehicle. As seen in (5.1), we can use both up-time, $t_{\text{on},i}$ and down-time $t_{\text{off},i}$ to get an accurate estimation. See Figure 5.4. This gives us two speed estimations, v_1 and v_2 of which we can take the average to form our estimated speed.

$$v_{\text{est}} = \frac{v_1 + v_2}{2} = \frac{1}{2}\left(\frac{d}{t_{2,\text{on}} - t_{1,\text{on}}} + \frac{d}{t_{2,\text{off}} - t_{1,\text{off}}}\right). \tag{5.1}$$

The estimation is affected by a difference in sensitivity [10]. The difference in sensitivity introduces a delay ε, assuming that the pulse is symmetric. This assumption is a good assumption for normal vehicles, but not for larger vehicles like buses and trucks - for these vehicles we need an ε_{on} and an ε_{off}. The estimated speed is now

$$v_{\text{est}} = \frac{1}{2}\left(\frac{d}{t_{2,\text{on}} - t_{1,\text{on}} + \varepsilon} + \frac{d}{t_{2,\text{off}} - t_{1,\text{off}} - \varepsilon}\right) \tag{5.2}$$

$$= \frac{d\left(t_{2,\text{on}} - t_{1,\text{on}} + t_{2,\text{off}} - t_{1,\text{off}}\right)}{(t_{2,\text{on}} - t_{1,\text{on}})(t_{2,\text{off}} - t_{1,\text{off}}) + \varepsilon\left([t_{2,\text{on}} - t_{1,\text{on}}] - [t_{2,\text{off}} - t_{1,\text{off}}]\right) + \varepsilon^2}. \tag{5.3}$$

The distance between sensors should be large, or equivalently the sampling frequency should be large in order to get accurate measurements. We also have the option to interpolate the signal since we are sampling at a frequency greater than twice the Nyquist frequency. A small distance

and high sampling frequency will get a average speed closer to the instantaneous speed. This information is often not required, and uses a lot of power since the AMR sensors consumes a lot of power, it is better to interpolate instead of oversampling. Sending information between nodes is also expensive.

If we can assume that all vehicles that passes the first sensor node also will pass the second sensor node, we can synchronise the data. In this case we also need to synchronise the time between sensor nodes, so that we will have accurate timestamps. Another solution is to put two magnetic sensors on each sensor node circuit board. This will allow us to use the same clock but the sampling frequency needs to be larger resulting in a higher power requirement.

Time difference using matched filter

A matched filter is a filter, h, that maximises the Signal-to-Noise Ratio (SNR) in the presence of additive stochastic noise.

$$y[n] = \sum_{k=-\infty}^{\infty} h[n-k]x[k], \tag{5.4}$$

where x is the indata, and y is the outdata. This filter can for example be used to find the synchronisation time in a communication system as illustrated in Figures 5.5a, 5.5b and 5.5c.

By choosing our matched filter as the time reversed output from the first sensor, we can find the time difference between the two similar outputs. The pulse shape should be chosen so that the matched filter output has a sharp peak as possible to not be affected as much by noise. Things that will affect the peak are for example distance to sensor, speed, sensor axis, and sampling frequency. By choosing the matched filter like this, we can see that it can be implemented in real-time and the peak is found when the vehicle has passed both sensors. With this algorithm, we can get subsample resolution by interpolation of the two signals. We can also interpolate around the peak of the convolution.

5.5.2 Average speed estimations

An average speed estimation for a number of vehicles can be done with a single sensor assuming we know the distribution of vehicle lengths [11]. Consider n vehicles with on-times $t_1, \ldots, t_n$ and lengths $l_1, \ldots, l_n$. Their unknown assumed common speed is $v = v_1 = v_2 = \ldots = v_n$. We have $n+1$ unknowns and n equations of the form

$$l_i = t_i v \quad i = 1, \ldots, n. \tag{5.5}$$

If we now know or assume the distribution of the vehicle lengths, we can obtain a maximum likelihood estimate of the vehicle speed $\hat{v}$ and also the vehicle lengths

$$\hat{l}_i = t_i \hat{v}, \quad i = 1, \ldots, n. \tag{5.6}$$

An estimate of the speed is then just

$$\bar{v} = \frac{\bar{l}}{\bar{t}}, \tag{5.7}$$

where $\bar{x}$ denotes the median value of that variable. The median length $\bar{l}$ is assumed to be 5 meters. The accuracy of this methods depends on the difference between the actual vehicle length and the value of $\bar{l}$.

If we use the speed estimate $\bar{v}$ for $\hat{v}$ in (5.6), we will get the vehicle length estimates [26]

$$\hat{l}_i = t_i \bar{v}, \quad i = 1, \ldots, n. \tag{5.8}$$

The number of vehicles, n, must be small enough for the assumption $v = v_1 = v_2 = \ldots = v_n$ to hold [26]. Alternatively we can define two new parameters [27] for each lane,

$$q = \frac{n}{T} \tag{5.9}$$

$$\theta = \frac{\sum_{i=1}^{n} t_i}{T}, \tag{5.10}$$

where q is the flow and θ is the occupancy. T is the time period length. Assuming that there is no correlation between vehicle length and vehicle velocity, we reach an estimate of the speed as

$$\hat{v} = \frac{q \cdot \hat{l}}{\theta}, \tag{5.11}$$

where $\hat{l}$ is assumed to be known and constant.

5.6 Classification

There are many methods for classification of vehicles. Older sensor systems has set the standard for what features in the sensor outputs are used. Traditionally when pressure tube measurements have been used, one could easily find the number of axles, and the distance between them, and the direction of travel. Sometimes – depending on the setup – one could also find in which lane the vehicle travelled Later, even when magnetic loop sensor was introduced, the classes were still basically light and heavy traffic although much research has been made in this area. We propose a system based on a classification scheme found in [24] for use with other sensors. This classification has seven classes, based on the information we can get from the AMR sensors. The seven used classes can be found in Table 5.1. The classification classes is different between different countries.

Table 5.1: *Vehicle classes [24]*

Class number	Type
1	Passenger car, mini-van, sports car, station wagon
2	SUV, pickup
3	Van, full-size pickup
4	Bus
5	Mini-truck
6	Truck
7	Other

For a random variable X or function $g(X)$ moments can be defined. The signature of a passing vehicle, i.e., the sensor output has properties that make these parameters usable. The moments can be used as parameters in the classification of vehicles. An example of this can be see in Figure 5.7. The kth central moment μ_k is defined [28] as

$$\mu_k = E[(X - \mu)^k], \tag{5.12}$$

where μ is the expectation value. The *skewness* γ_1 and *kurtosis* γ_2 are defined as

$$\gamma_1 = E\left[\left(\frac{(X-\mu)}{\sigma}\right)^3\right] \tag{5.13}$$

$$\gamma_2 = E\left[\left(\frac{(X-\mu)}{\sigma}\right)^4\right] - 3. \tag{5.14}$$

For the normal distribution $\gamma_1 = \gamma_2 = 0$. The skewness and kurtosis are estimated as

$$\hat{\gamma}_1 = \frac{1}{n}\sum_{1=i}^{n}\left(\frac{x_i-\mu}{s}\right)^3, \tag{5.15}$$

$$\hat{\gamma}_2 = \frac{1}{n}\sum_{1=i}^{n}\left(\frac{x_i-\mu}{s}\right)^4 - 3, \tag{5.16}$$

where s is the estimated standard deviation.

A distribution having a longer tail at earlier times, i.e. the "left side" of the signature distribution, then it is negatively skewed and vice versa. If the tails are thinner than those of the normal distribution it has positive kurtosis.

5.6.1 Tree method

Significant pre-processing of the raw data is required [11] for this method. The signal magnitude needs to be normalised, the on-time must be converted into length by multiplying with the speed and every data set must be re-sampled to the same number of samples. The decision method is then based on a decision tree which can be seen in Figure 5.7. A number of thresholds, b_i, are chosen which are related to signature length, signature magnitude and skewness. The thresholds can be chosen at design time or more intelligently by training the sensor. The thresholds are then used in a greedy best-first search in the tree seen in Figure 5.7.

If the sensors are placed in the center of the lane the signatures will be very different compared to when the sensors are placed at the side of the road. They will show more distinct features and by using a basic thresholding algorithm, we can classify them using a tree in the same way as above. We will receive a pattern consisting of ± 1 that will have different lengths depending on the vehicle. If we instead of the thresholds b_i use a single threshold we can define this pattern. Now we proceed in the same manner as before using the decision tree in Figure 5.7. The bit pattern can be defined as

$$\overline{c(n)} = \begin{cases} +1 & x(nT_s) \geq c_+ \\ -1 & x(nT_s) < c_- \\ 0 & \text{otherwise,} \end{cases} \tag{5.17}$$

where $x(nT_s)$ is our sampled signal. The bit pattern can be compared to a database somewhere in the network and the closest match determines the vehicle class. An example can be seen in Figure 5.6.

5.6.2 Hill patterns

Another way of finding a pattern like the one described in the previous section is to use hill patterns. These are found exactly in the same way as the pattern above, but using the time

derivative of the signature. This method has the benefit that we do not need to place the sensor in the middle of the lane but rather at the side of the road. Noise will be an issue with this method, and therefore the signal will need filtering.

The hill pattern is defined [10] as

$$d(n) = \frac{x(nT_s) - x([n-1]T_s)}{T_s}, \quad n \in \mathbb{Z} \tag{5.18}$$

$$\overline{d(n)} = \begin{cases} +1 & d(n) \geq d_+ \\ -1 & d(n) < d_- \\ 0 & \text{otherwise,} \end{cases} \tag{5.19}$$

where d_+ and d_- are the thresholds, positive and negative respectively. Normally they are chosen so that $d_+ = -d_-$.

5.6.3 Transforms

Algorithms based on on discrete Fourier transform, DFT, and Karhunen-Loève transform, KLT, are proposed in [24]. In Appendix A we can find the Fast Fourier Transform, FFT, of the vehicle signatures in each axis. The sensor was placed at the side of the road. We can see that the signatures contain a very different frequency content, and therefore classification could be done using FFT.

5.6.4 Bins

If we do the normalisation and re-sampling as in earlier methods, we can divide the signature into bins. Two examples can be seen in Figures 5.8a and 5.8b. We take the mean of the magnitudes in a number of time slots and so we have produced a vector that can be compared with a database. The number of time slots are the same for all vehicles, but the length of each time slot might be different. The length of a signature is an important parameter, and therefore it is necessary to measure that parameter in some way. One way could be to always "record" the same signature length, or pad with zeros after the vehicle has passed. Of course we could compare the signature itself with the database entry, but this would require the whole signature to be sent over the WSN, which would perhaps not be effective.

5.6.5 Least-squares estimation

Using least squares analysis we seek to minimise (5.20) in order to find the parameters of the magnetic model. This method although very good requires extreme computational power.

$$S = \sum_i^n \left(y_i - f(\boldsymbol{t}_i, \boldsymbol{a})\right)^2, \tag{5.20}$$

where y_i is the measured data, $f(\boldsymbol{t}_i, \boldsymbol{a})$ is the output from our model described in Chapter 4 and $\boldsymbol{a}$ is a vector containing the parameters we want to estimate. $\boldsymbol{t}_i$ is the time samples, n is the number of samples we have.

The parameters estimated are

$$\boldsymbol{\mu}_i = [\, \mu_{x,i} \quad \mu_{y,i} \quad \mu_{z,i} \,] \tag{5.21}$$

$$\boldsymbol{r}_i = [\, x_i \quad y_i \quad z_i \,], \tag{5.22}$$

and also the speed v. It is assumed that the magnetic moments will lie on a straight line, eliminating two degrees of freedom. The vehicle is assumed to be travelling a path perpendicular to the sensor. Three magnetic moments each with four degrees of freedom will have a total of twelve degrees of freedom. Placing one of the magnetic moments in the origin of the vehicle coordinate system will eliminate another degree of freedom. Since the vehicle coordinate system will move, we can add the speed v as another parameter. In all, twelve parameters are estimated from measurements.

5.7 Queue Detection

A queue is a number of vehicles that travel slowly close together. This tells us that we can define a function $q(v, d) \geq 0$ where v is the average velocity, and d is the mean distance between vehicles. We can then set a threshold for a function $q(v, d) \in \{0, 1\}$ below which we have a queue. A value of 0 means that there are no vehicles on the road, a value of 1 means that the road is completely filled with still-standing vehicles. The mean speed and distance between vehicles can be found in different ways. We can also just see how often the sensor is "occupied". A high occupancy means a large number of vehicles, or few slow moving vehicle. We also note that if we are interested in minimising the number of "catching-up accidents", just one vehicle is enough to make a very dangerous situation, and therefore it is enough to detect one slow-moving or parked vehicle.

In a queue detection system the nodes need to be complemented by a warning unit. A number of these are presented in Appendix D including a flashing unit from Amparo SeeMe™.

No performance analysis will be done for queue detection since velocity estimation forms the basis for queue detection. However, if queue detection will be used the threshold for the $q(v, d)$ function needs to be trimmed in so that we are not sending a warning too often, or too seldom.

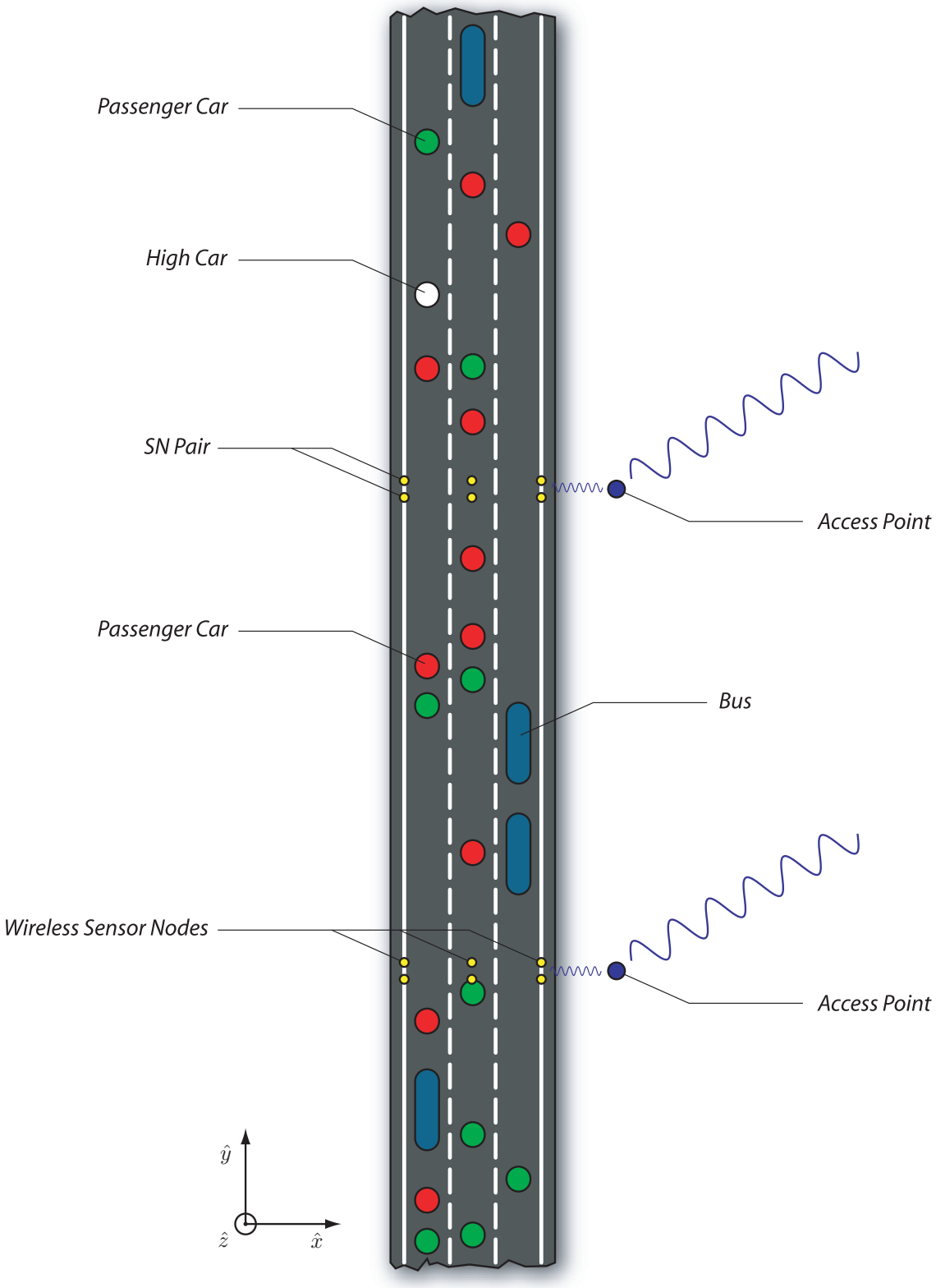

Figure 5.1: *System overview. Road surface with cars and buses. SNs are placed in pairs to estimate speed. Note the in-lane sensors and the roadside sensors. APs send the information to the backbone.*

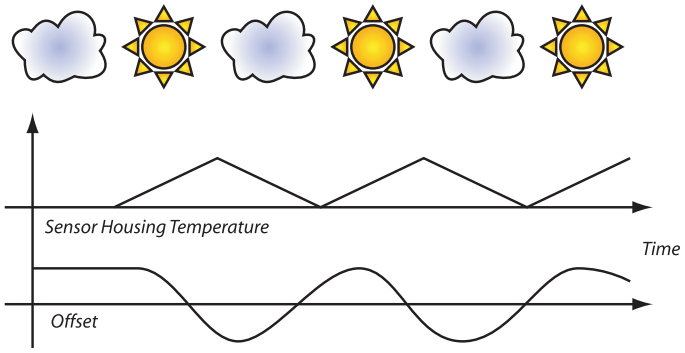

Figure 5.2: *Offset depending on temperature*

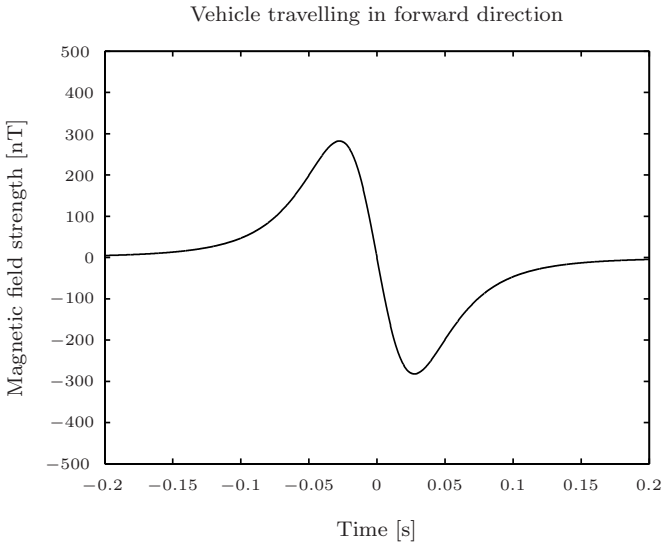

Figure 5.3: *Direction finding using one sensor. Vehicle travelling in forward direction. If the vehicle backs up, the signature looks like a mirror image. Note that the signature depends on the sensor position.*

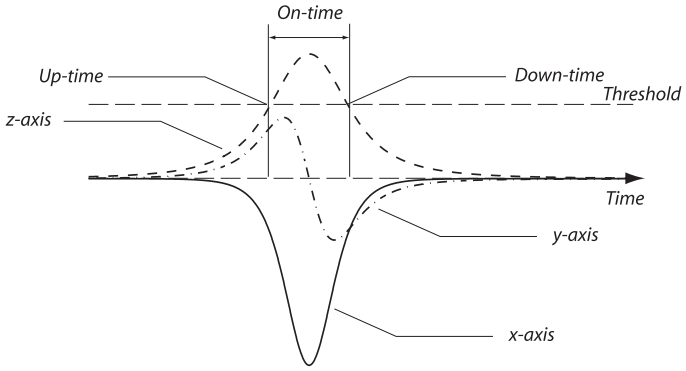

Figure 5.4: *Parameters for speed estimation. Up time is the arrival time of the vehicle. Off time is the departure time. On time is the difference between the two first.*

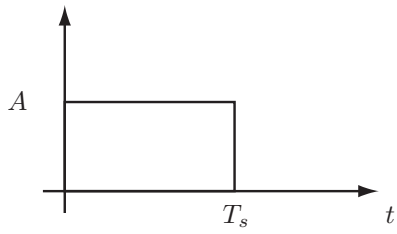

Figure 5.5a: *Synchronisation pulse. This is the pulse that we are looking for using the matched filter.*

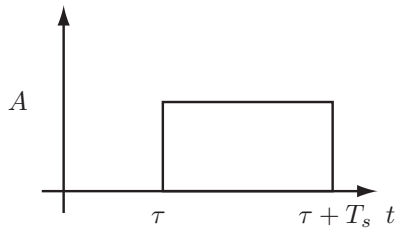

Figure 5.5b: *Measured data. This is basically a delayed version of the first signal.*

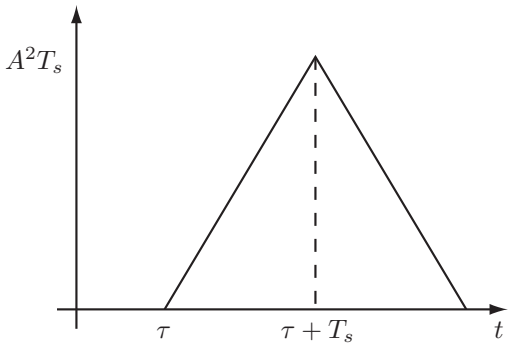

Figure 5.5c: *Convolution between the signals. The peak will be located at $T_s + \tau$.*

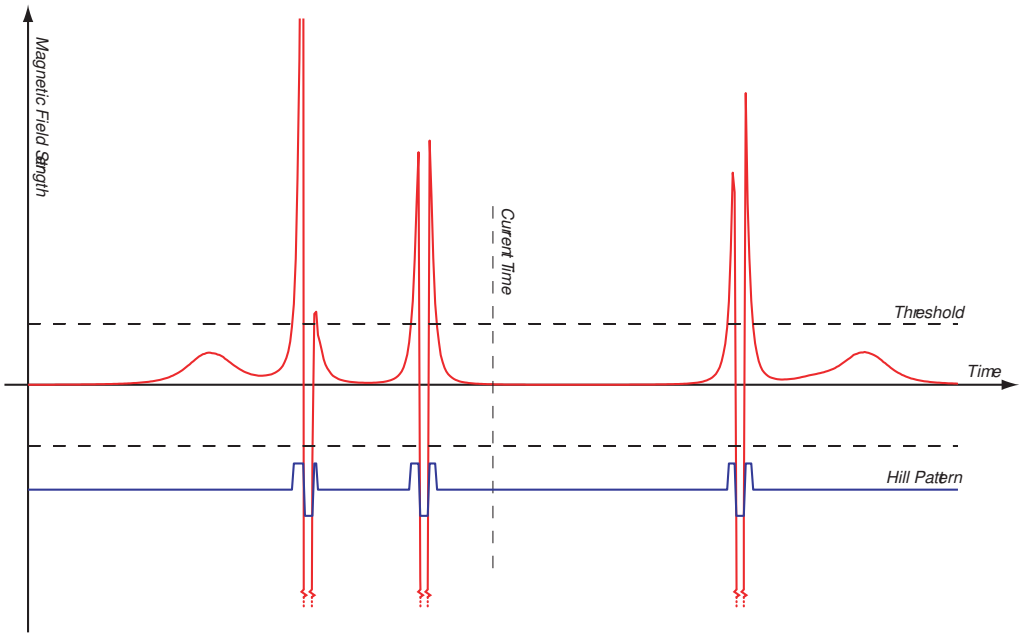

Figure 5.6: *Sensor data and pattern.*

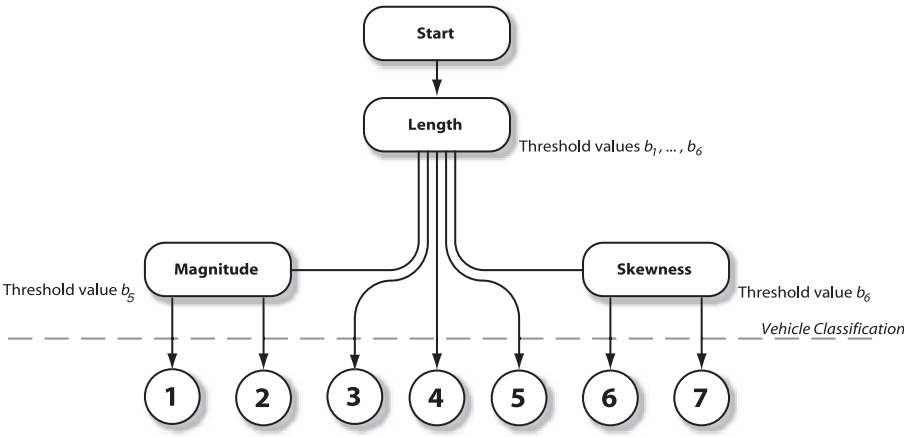

Figure 5.7: *Decision tree for classification into seven types of vehicles [24].*

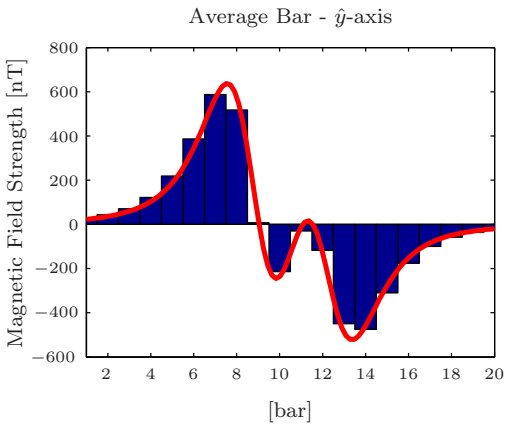

Figure 5.8a: *Average bar - y-axis.*

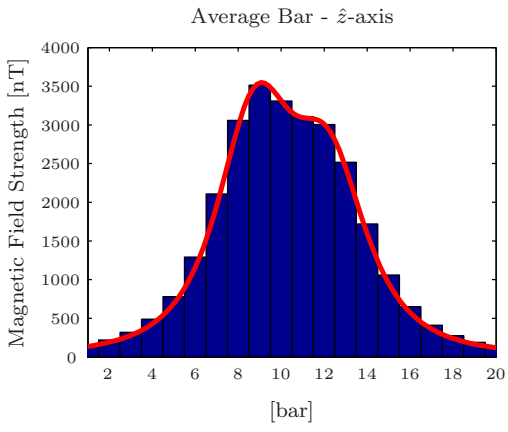

Figure 5.8b: *Average bar - z-axis.*

Chapter 6

Performance analysis

6.1 Sensor placement

6.1.1 Translation

The general rule about sensor placement is that the closer the sensors are to each other, the more accurate the placing has to be. For example at the desired inter-sensor distance 2 m, a misplacement of 5 cm yields a 2.5 % error in velocity. At the desired inter-sensor distance 0.2 m, a misplacement of 5 mm yields the same error. Since it is complex to sample too often, and by only considering sensor placement, the nodes in a sensor pair should be placed as far from each other as possible.

6.1.2 Rotation

When placing the sensor it is important that the axes point in the correct directions. However it is easy to accidentally rotate the sensor. The effect of rotating the sensor in the yaw ($\hat{z}$) and pitch ($\hat{y}$) axes can be seen in Figures 6.1a and 6.1b. If the rotation is known the software could easily correct for this.

6.2 Detection

In the simulator a number of potential problems have been identified. If two vehicles are travelling close to each other, especially if they are large, the signal will be indistinguishable from a single very long vehicle. This can be combated by placing the sensor as close to the vehicles as possible. Similarly, a vehicle in an adjacent lane will disturb our signal. This is remedied by choosing the threshold value wisely. Some vehicles such as motorcycles and some small cars will not produce a signal with high enough magnitude. Placing the sensor closer to the vehicle will help, more sensors will ensure that the vehicle pass at least one sensor.

In the real-life tests performed, we detected 100 % of normal-sized vehicles. The vehicles not

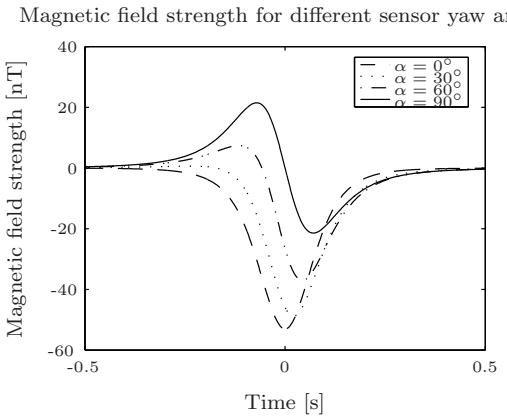

Figure 6.1a: *Effect of sensor node rotation. The sensor is rotated around its yaw axis and the effect on the $\hat{\boldsymbol{x}}$-axis can be seen.*

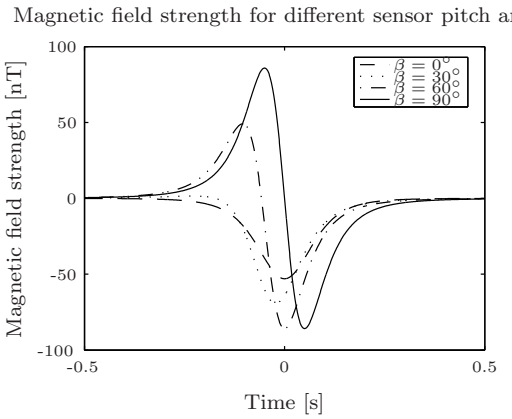

Figure 6.1b: *Effect of sensor node rotation. The sensor is rotated around its pitch axis and the effect on the $\hat{\boldsymbol{z}}$-axis can be seen.*

detected were bicycles and a very small motorcycle. The signature from each vehicle was clearly visible, and could be both seen by eye or by a simple counting algorithm. The simulations displayed very similar vehicle signatures, but not all vehicles were detected due to the minimum distance between vehicles set in the simulator. In the real life test there were no vehicles travelling bumper to bumper which was expected due to the comparably high speed.

6.3 Speed estimation

6.3.1 Speed of an individual vehicle

Traditional time difference

$$v_{\text{est}} = \frac{d\left(t_{2,\text{on}} - t_{1,\text{on}} + t_{2,\text{off}} - t_{1,\text{off}}\right)}{(t_{2,\text{on}} - t_{1,\text{on}})(t_{2,\text{off}} - t_{1,\text{off}}) + \varepsilon\left([t_{2,\text{on}} - t_{1,\text{on}}] - [t_{2,\text{off}} - t_{1,\text{off}}]\right) + \varepsilon^2}. \tag{6.1}$$

The term $\varepsilon\left([t_{2,\text{on}} - t_{1,\text{on}}] - [t_{2,\text{off}} - t_{1,\text{off}}]\right)$ in (6.1) is small if the signature is equal or similar at both sensors. In contrast to the conclusion in [10], the term ε^2 is small, but not zero. If we assume a sampling speed of 100 Hz, a velocity of 72 km/h, a sensor separation of 2 m and $\varepsilon = 2$ samples then the sensitivity parameter ε^2 introduces an error of 4 %. If the distance is doubled, the error is 1 %. The speed is a factor, a higher speed means less accuracy – see Figure 6.2.

Comparison between traditional time difference and time difference using matched filter

A comparison between the traditional and matched filter methods can be found in Figures 6.3a, 6.3b, 6.4a, 6.4b, 6.5a and 6.5b. In Figures 6.6b and 6.6b we can see the result if we use the Euclidean norm $\|\boldsymbol{B}\| = \sqrt{B_x^2 + B_y^2 + B_z^2}$. We can see that the standard deviation of the matched filter (MF) method is much smaller than the standard deviation for the traditional method, or peak to peak (P-P) method regardless of SNR and sensor axis. We can see that the use of a lowpass filter (LP) on the first signal introduces an expected delay into the system. This filtering

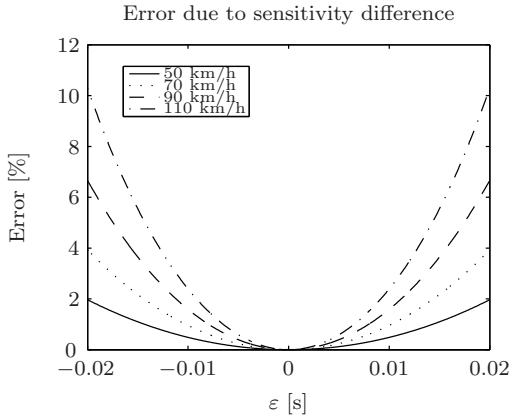

Figure 6.2: *Time difference. Error due to sensor sensitivity difference. The distance between sensors was 2 m, and the speed was 20 m/s.*

is done since we know we are not looking for an exact replica of the first signal and its noise, but rather a copy of the first clean signal with added, different, noise. This delay is of course known and can be compensated for. A lowpass filter will cause the time difference to be underestimated, and therefore the speed will be overestimated. We also note that it is beneficial to use the more complex y-axis.

For all of these simulations, the sensors were placed 1.5 m from the passing vehicle, and the SNR was varied between ~ 0 dB and 40 dB. The vehicle speed was 72 km/h.

If we plot the mean error and error standard deviation versus the speed, we will see that the error and the error standard deviation goes to zero at higher speeds for the matched filter method. The result can be seen in Figures 6.7a and 6.7b.

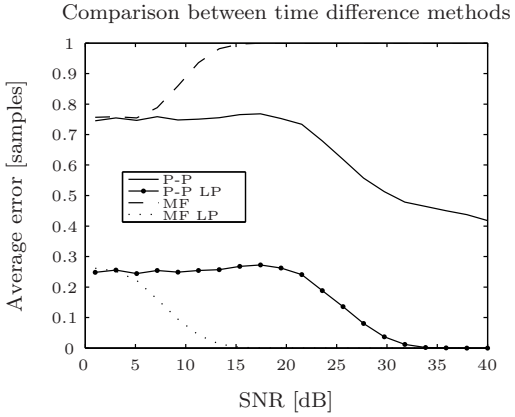

Figure 6.3a: *Comparison between traditional and matched filter methods. Mean error versus SNR. The sensor is placed 1.5 m from the vehicle and on the road surface. The sensor output in $\hat{z}$-axis has been used.*

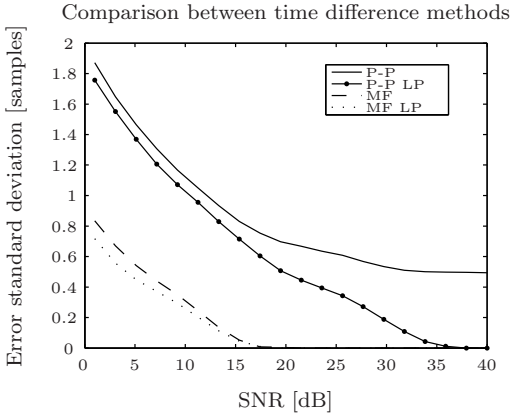

Figure 6.3b: *Comparison between traditional and matched filter methods. Standard deviation versus SNR. The sensor is placed 1.5 m from the vehicle and on the road surface. The sensor output in $\hat{z}$-axis has been used.*

Peak-to-peak time difference has a higher mean error than the matched filter method for low noise situations. We can see in Figure 6.3a how the lowpass filter introduces a delay. Both methods has the same error in case of high noise. Note that due to the sampling strategy, the matched filter methods seem to have a mean error of one sample. This error is a product of the implementation,

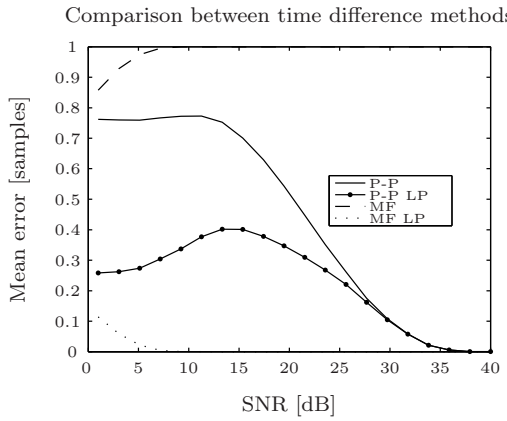

Figure 6.4a: *Comparison between traditional and matched filter methods. Mean error versus SNR. The sensor is placed 1.5 m from the vehicle and on the road surface. The sensor output in $\hat{y}$-axis has been used.*

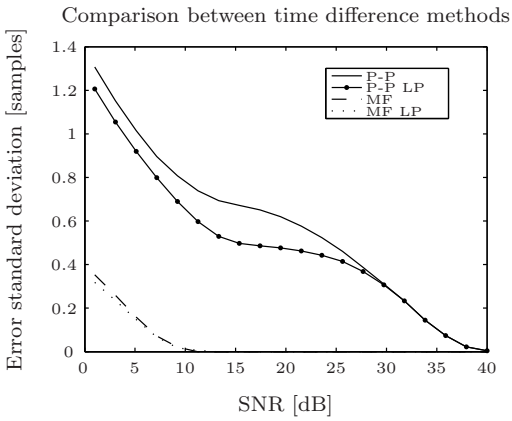

Figure 6.4b: *Comparison between traditional and matched filter methods. Standard deviation versus SNR. The sensor is placed 1.5 m from the vehicle and on the road surface. The sensor output in $\hat{y}$-axis has been used.*

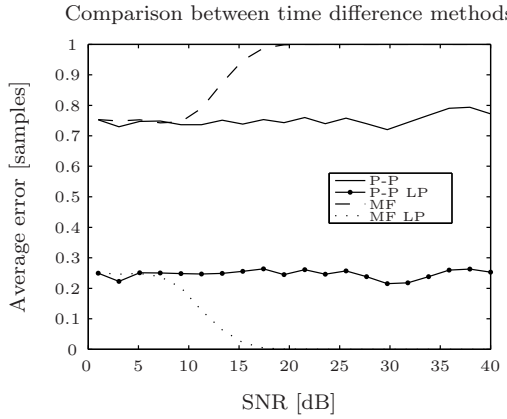

Figure 6.5a: *Comparison between traditional and matched filter methods. The vehicle was a bus. Mean error versus SNR. The sensor is placed 1.5 m from the vehicle and on the road surface. The sensor output in $\hat{z}$-axis has been used.*

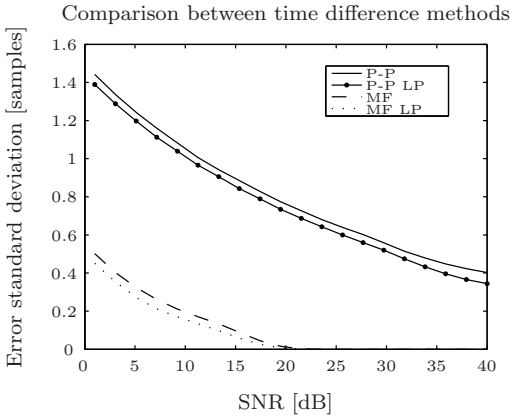

Figure 6.5b: *Comparison between traditional and matched filter methods. The vehicle was a bus. Standard deviation versus SNR. The sensor is placed 1.5 m from the vehicle and on the road surface. The sensor output in $\hat{z}$-axis has been used.*

the error actually goes to zero. In this case the error always goes to one, so it is predictable, and therefore has no impact. The P-P has a much higher standard deviation than using matched filter. We can see how the LP filter reduces standard deviation in both cases but not by much. The recommendation is to use matched filter without LP filter.

The benefit of using the matched filter method is clearly better estimation of the time difference. However, the disadvantage of this method is that the matched filter requires knowledge of both signals and therefore more information has to be sent over the network. We should note that these calculations can be done in close to real-time, and the decision can be taken when the vehicle has passed both sensors.

With a more complex signal, as seen in Figures 6.5a and 6.5b the error goes to zero faster for the matched filter method. This means that we should choose the most complex axis or a combination of axes when using this algorithm. We can also see that since a higher vehicle velocity will give

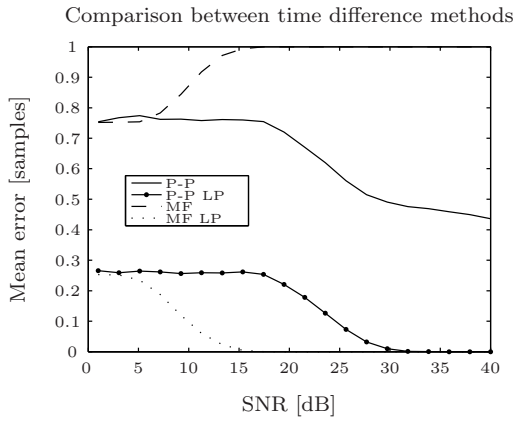

Figure 6.6a: *Comparison between traditional and matched filter methods. Mean error versus SNR. The sensor is placed 1.5 m from the vehicle and on the road surface. The norm of the sensor output has been used.*

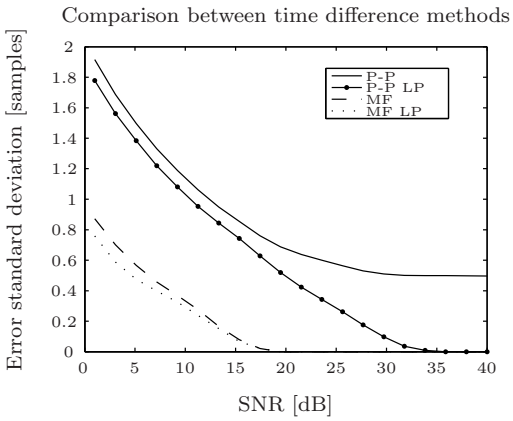

Figure 6.6b: *Comparison between traditional and matched filter methods. Standard deviation versus SNR. The sensor is placed 1.5 m from the vehicle and on the road surface. The norm of the sensor output has been used.*

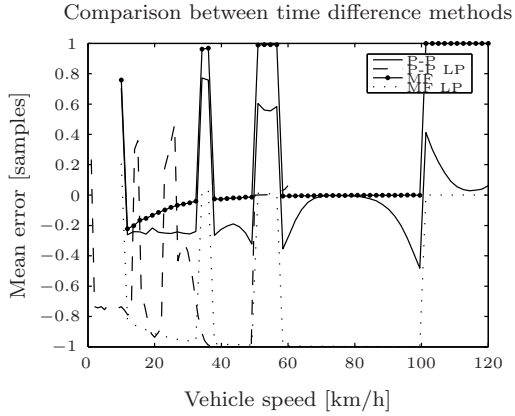

Figure 6.7a: *Comparison between traditional and matched filter methods. Mean error versus velocity. The sensor is placed 1.5 m from the vehicle and on the road surface. The sensor output in $\hat{z}$-axis has been used.*

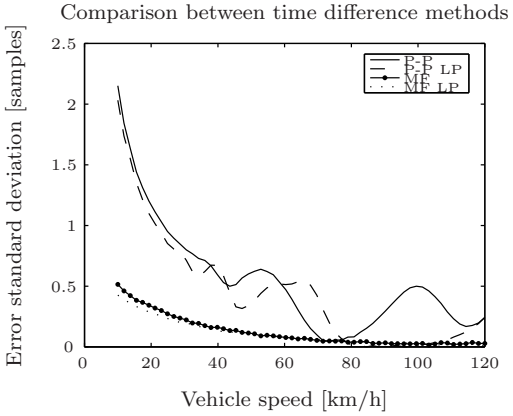

Figure 6.7b: *Comparison between traditional and matched filter methods. Standard deviation versus velocity. The sensor is placed 1.5 m from the vehicle and on the road surface. The sensor output in $\hat{z}$-axis has been used.*

us sharper peaks, the error becomes smaller with greater speeds. The standard deviation also becomes smaller. Note that graphs are plotted versus SNR and that the signal amplitude is different for different vehicles and axes.

One important aspect of this algorithm is that it is not affected by the difference in sensitivity as the traditional algorithm is.

The SNR is defined as

$$\lfloor \mathrm{SNR} \rfloor_{\mathrm{dB}} = 10 \log \left(\frac{\langle x^2(t) \rangle}{\sigma^2} \right), \tag{6.2}$$

where $\langle x^2(t) \rangle$ is the mean of the square of our signal as

$$\langle x^2(t) \rangle = \frac{1}{n} \sum_{i=1}^{n} x_i^2, \tag{6.3}$$

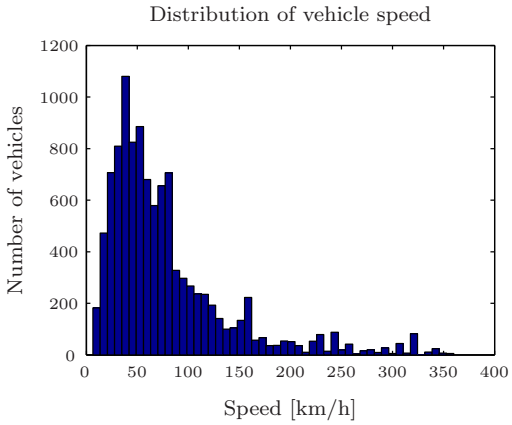

Figure 6.8: *Estimated speed using the occupancy method from Section 5.5.2. True speed was 72 km/h and only passenger cars were used. Mean speed was* 78.6 *km/h and median speed was* 60.4 *km/h. Vehicles with speed over 360 km/h was discarded. The total number of remaining vehicles was 8642 and* $\hat{l}$ *was chosen to be 4.5 m. Adjusting this parameter will shift the distribution. The time interval was 10 seconds.*

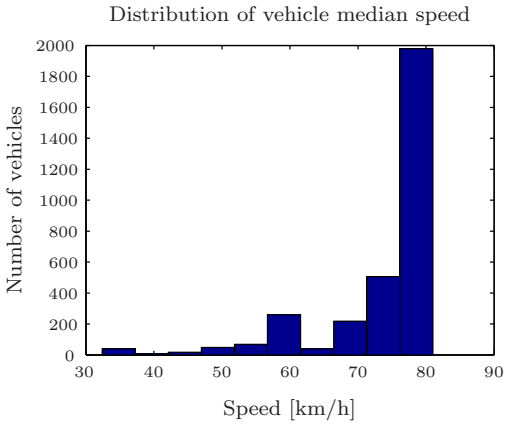

Figure 6.9: *Estimated speed using the median velocity method from Section 5.5.2. The true speed was 72 km/h, mean speed was* 73.8 *km/h and the median speed was* 77.1 *km/h. Standard deviation was* 8.95 *km/h. The total number of vehicles was above 3000.* $\hat{l}$ *was chosen to be 4.5 m. Adjusting this parameter will shift the distribution. Note the over estimation due to* $\hat{l}$ *and the shape of the distribution.*

if $x_i(t)$ is a discrete function with n samples. σ is the standard deviation of the Gaussian noise. For the plots in this section, the SNR of the signal from the first sensor has been used. If we have used another reference signal, we will get $\langle x_1^2(t) \rangle = \alpha \langle x_2^2(t) \rangle$ where α is a factor. Due to the nature of logarithms, this will only introduce an offset.

If sensors are placed in pairs with one master and one slave, the master is responsible for uploading the measured data to the system. Due to the asymmetric power consumption between master and slave, it might be better to upload all data to the access point before processing.

6.3.2 Average speed estimations

A simulation result of the occupancy method can be seen in Figure 6.8. We can deduce from the histogram that the standard deviation is quite large for this method.

In Figure 6.9 we can see the result from the median speed method. The fact that the method over estimates the speed can be corrected for by adjusting the $\hat{l}$ parameter. The standard deviation was 8.95 km/h or 5.57 mph which is somewhat larger than the reported 2.5 mph standard deviation for a 10-point median speed estimation in [11].

6.4 Classification

The classification schemes are very different depending on sensor positions. In the limited simulations done we have found the classification rate to be nearly 100 % when the sensor is placed in the roadway. The classification has been done in three classes; Passenger cars, SUVs (high cars) and buses. A classification accuracy of 60 % has been reported [11] not using length as a feature.

Using the two sensors in a pair will of course make the classification more accurate, especially since we then can use the speed estimation to estimate the vehicle length.

Since it is expensive to install sensors in the roadway, we have decided to only use sensors at the side of the road. A roadside sensor position make classification much more difficult. Due to the signature properties, we can use the derivative of the signal to increase the accuracy. This method is more sensitive to noise, and requires filtering of the signal.

We can also look at the transform of the signal, for example the FFT. The FFT of different vehicle signatures can be seen in Appendix A. These transformed signals show potential to be used for classification, although it will need further investigation.

6.4.1 Estimation of model parameters

One method of classification is trying to estimate the parameters that we use in our model, and compare the results to our database of vehicles. The database that we are using does not contain enough data to give a good analysis of the relability of the method but we can use the method for a proof of concept.

When using the least-squares estimation method described in Section 5.6.5 we obtain the results than can be seen in Figure 6.10b. The measured data can be seen in Figure 6.10a.

The parameters estimated are as earlier stated

$$\boldsymbol{\mu}_i = [\, \mu_{x,i} \quad \mu_{y,i} \quad \mu_{z,i} \,] \tag{6.4}$$

$$\boldsymbol{r}_i = [\, x_i \quad y_i \quad z_i \,]\,. \tag{6.5}$$

It is assumed that the magnetic moments will lie on a straight line in the center of the vehicle thereby eliminating two degrees of freedom. The vehicle is furthermore assumed to be travelling a straight path perpendicular to the sensor. Since the vehicle coordinate system will move, we can add the speed v as another parameter. In all, twelve parameters are estimated from measurements.

The estimated data and measured data almost match in shape, but not in amplitude. The most interesting thing we can see from this estimation is that in an estimation of three different magnetic moments for a passenger vehicle, two of the magnetic moments are very close in position and has opposite signs in at least two axes. This means that our model of using only one magnetic moment is probably a good model. An estimation with only one estimated magnetic moment can be seen in Figure 6.10c. The discrepancy is in both estimation due to a number of unknown parameters in the measurements done by Imego, however we can still see the similarity. Among those parameters are the distance to the sensor and the vehicle velocity.

6.5 Verification of algorithms

Measurements done with our prototype node can be seen in Figure 6.11a. The frequency content can be seen in Figure 6.11b. The signal contains a lot of power around 50 Hz which is expected. Noteworthy is that the signal contains most of its power at very low frequencies, and therefore we can use a crude filter to get rid of the noise at higher frequencies. The influence of the 50 Hz frequencies was later made smaller by the use of a 2nd order IIR notch filter. We can see that the vehicle signatures are much higher in amplitude than the noise. The large signature in the data in Figure 6.11a comes from a large double-deck bus.

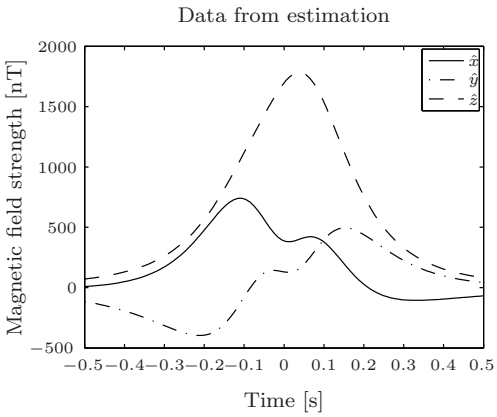

Figure 6.10a: *Data from estimated parameters. Three magnetic moments were estimated. Note the different time scale.*

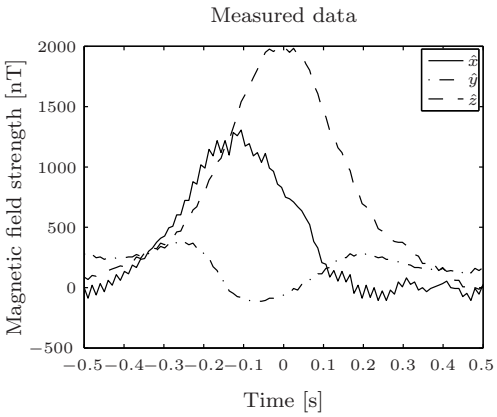

Figure 6.10b: *Measured data from passing vehicle.*

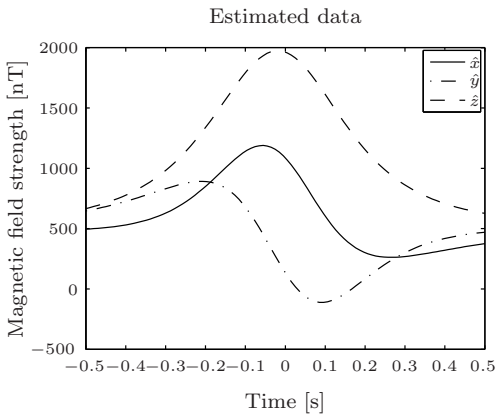

Figure 6.10c: *Data from estimated parameters. One magnetic moment was estimated.*

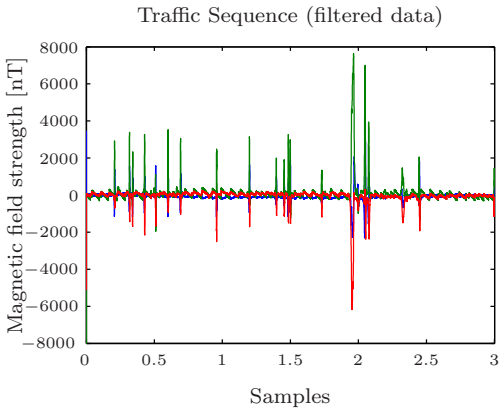

Figure 6.11a: *Measured data from traffic. The signal was filtered using a low order digital low-pass filter.*

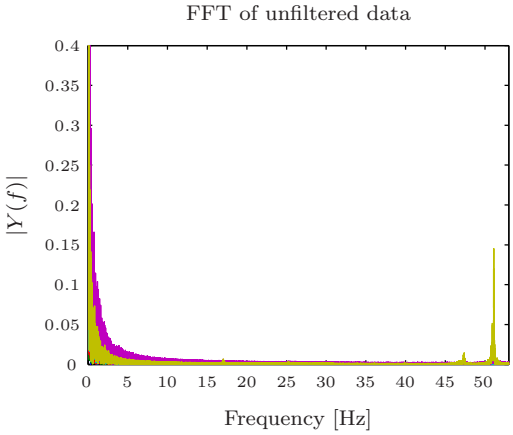

Figure 6.11b: *FFT of measured data from traffic. Unfiltered data.*

It is worth noting that if we have traffic travelling in the other direction, we can eliminate them using their speed estimation. Of 18 vehicles travelling in the positive direction, 18 are detected.

This is of course a very short sample, and more measurements have to be done. If a driver is instructed to pass the sensors at 50 km/h, the result differs from that velocity by a maximum of 2 km/h when the matched filter method was used. The number of vehicle passings was only thirteen. Due to the limited use of the experiment data, a velocity control measurement was deemed necessary.

The most energy in the signal can be found at low frequencies which means that we can use a low pass filter to get rid of undesired high frequency content.

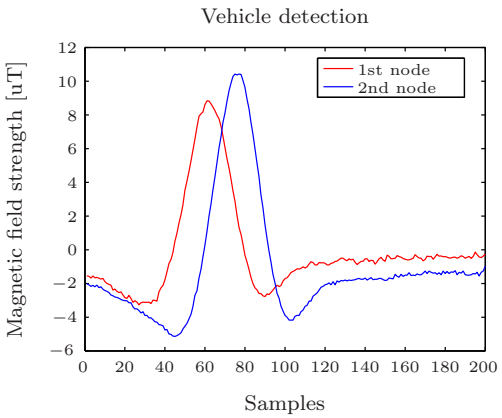

Figure 6.12a: *Two-node vehicle detection. The distance between the curves determine the speed of the vehicle.*

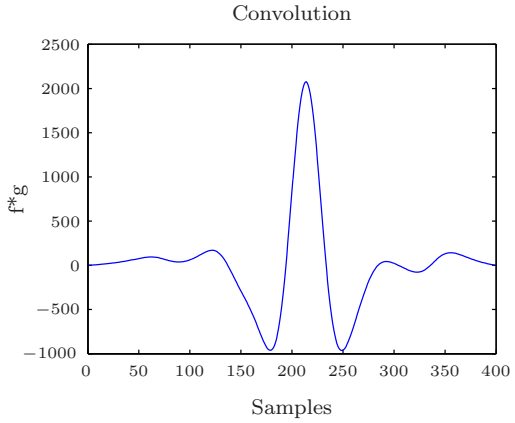

Figure 6.12b: *Convolution of the first and second node data. The peak is clearly visible.*

The result of the convolution of the two sensor node outputs seen in Figure 6.12a can be seen in Figure 6.12b. We can see that the peak is well defined, and not noisy. In fact, the sensor node signals can be much more noisy as described earlier. An example of an interpolation around the peak can be seen in Figure 6.13.

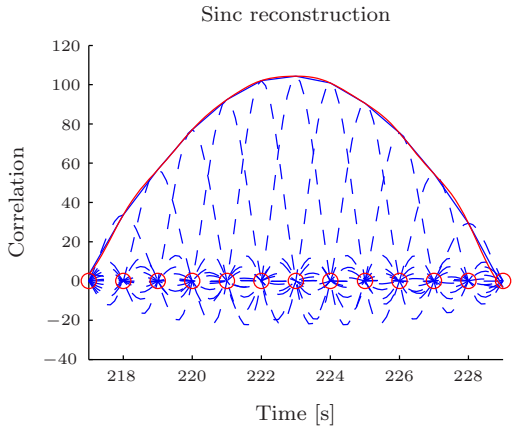

Figure 6.13: *Sinc reconstruction of the convolution peak.*

In the result we can see that the estimated speeds do not differ by much when we use different sensor axis. We also note that the difference in sensor sensitivity does contribute in the sense that we have to use a different threshold but not otherwise. This is a huge improvement over the peak to peak method used in other publications.

Chapter 7

Discussion

7.1 Model validity

The model of the earth magnetic field used in this thesis is a very crude and simple model, however these simplifications are necessary due to the tremendous complexity of the magnetic field and for computational reasons. The impact of these simplifications are such that they will give us a slightly different field. A different field will induce different magnetic dipole moments in a vehicle, and since it is impossible to know the field at all positions at all times we have to make these simplifications. Places where problems occur include high current cables, tunnels and some geographic positions such as the poles. Thankfully not much traffic exist at the poles.

Parameters such as vehicle acceleration, different vehicle positions on the road, different cargo, different car models will have a huge impact on the signal. Some of these can be tested in the simulator, but measurements have to be done for verification. Since the evaluation is simulation based, we will always have to do a lot of simplifications. Other parameters that affect the result are quantisation, electronic noise, synchronisation mismatch and inhomogeneous sampling frequency.

7.2 Algorithm validity

It is imperative that the algorithms are evaluated using real data because of the simplification discussed in the previous section. Given our current location, and the simplifications done in the simulator, we can safely say that the algorithms apply at least to the four different vehicles modelled. We now make an assumption, that these algorithms will apply to all vehicles according to the inductive approach used in this thesis.

A problem in the measurements is that when drivers see the sensor nodes they tend to swerve and the distance to the sensor is therefore not constant during the passing of a vehicle. It is also not constant between different vehicles making the processing of the data more difficult. However the data is still usable, and a if a live system will see better data it will perform better according to the old saying “train hard – fight easy”.

Chapter 8

Conclusion

In this thesis evaluations of sensor algorithms were performed. The primary questions we wanted to answer was if a WSN system was suitable for

- **traffic monitoring**, i.e. primarily counting, speed estimation and classification,
- **queue detection**, i.e. speed estimation and presence.

The thesis shows that a WSN can be used for detection of vehicle presence, counting vehicles, estimating individual and average speeds, and classification of vehicles. Furthermore it shows that the performance of such a system is within acceptable limits. A problem is however that the sensors are not power efficient enough for an application where long battery life is critical. The thesis does not prove that such a system or the design of it is optimal in any way.

8.1 Theoretical model

We have seen that the sensor output matches the model, in some cases better than other. For the application of classifying vehicles, further work is needed. Vehicles can be classified manually, their magnetic properties can be catalogued and used in the system.

8.2 Hardware

It is concluded that speed should be estimated using two sensor nodes and therefore a sensor node should contain one AMR sensor. In general more axes mean better result, and more axes also provides the possibility to correct for errors due to rotation of the sensor node. The magnetic field will be different in different locations, and therefore one cannot be sure which axis is the best to use at a given location. The nodes should also include a temperature sensor so the magnetic sensor threshold can easily be adjusted. A temperature sensor will also give additional data for other purposes, or for warning vehicles for dangerous road conditions.

The sensors nodes should be placed in pairs with one three-axis AMR sensor each. The inter-sensor distance should be less than one vehicle length but as large as possible in order to maximise

speed estimation accuracy.

8.3 Algorithms

For detection an adaptive threshold algorithm should be used. The threshold should be set according to disturbing traffic, and sensor position. The threshold will need to be changed when conditions and temperature change.

Speed detection requires two sensors spaced at most one vehicle length apart in order to avoid problems with vehicles turning, changing lanes etc. It is therefore logical to place sensors in pairs.

The method of using matched filter compared to finding the peak to peak time difference is a very good method. It is not very sensitive to noise, and it can be used almost in real-time. The drawback is of course that the complexity and the network load will increase. A very important fact is that it does not depend on the difference in sensor sensitivity which is a huge improvement over earlier methods.

8.4 Future Work

The algorithms evaluated and used in this thesis need to be evaluated in real traffic conditions, only then can one be sure of the performance of the different algorithms. The complexity of these algorithms need to be studied before implementation and design in sensor nodes. The power consumption will depend heavily on how much information is sent over the wireless network.

The sensor properties need to be further investigated, especially regarding noise, temperature dependence, sensor casing properties and transceiver properties. The network properties also need investigating.

Choosing a threshold adaptively is difficult – the threshold should be chosen to be large enough to be higher than the noise and signals from disturbing vehicles. The algorithms for this should be investigated further.

Bibliography

[1] European Commission, "White Papers, European Transport Policy for 2010: Time to Decide," Luxembourg, 2001. [Online]. Available: http://europa.eu.int

[2] H. Linell and L. Nilsson, "Amparo Solutions AB, Company Presentation," Powerpoint, January 2007.

[3] H. Karl and A. Willig, *Protocols and Architectures for Wireless Sensor Networks.* Hoboken, USA: John Wiley and Sons Ltd., 2005.

[4] "Reconfigurable Ubiquitous Networked Embedded Systems (RUNES)," Internet, September 2007. [Online]. Available: http://www.ist-runes.org

[5] S. Arrigault and V. Zacharaki, "Design of a ZigBee Magnetic Sensor Node," Master's thesis, Chalmers tekniska högskola, Göteborg, Sweden, June 2007.

[6] I. C. Society, "802.15.4, Wireless Medium Access Control (MAC) and Physical Layer (PHY) Specifications for Low-Rate Wireless Personal Area Networks (LR-WPANs)," October 2003. [Online]. Available: http://standards.ieee.org/

[7] ZigBee Standards Organization, "ZigBee Specification," Internet, December 2006. [Online]. Available: http://www.zigbee.org

[8] M. Rydström, A. Urruela, E. G. Ström, and A. Svensson, "Autonomous Position Techniques Based on Cramér-Rao Lower Bound Analysis," in *EURASIP Journal on Applied Signal Processing*, no. 93043. Hindawi Publising Corporation, 2006, pp. 1–10.

[9] S. Y. Cheung, S. C. Ergen, and P. Varaiya, "Wireless Sensor Networks for Measuring Traffic," Powerpoint, Internet, November 2005. [Online]. Available: http://paleale.eecs.berkeley.edu/~varaiya/

[10] S. Y. Cheung and P. Varaiya, "Traffic Surveillance by Wireless Sensor Networks: Final Report for PATH TO 5301," University of California, Berkely, Tech. Rep., January 2007. [Online]. Available: http://www.path.berkeley.edu/PATH/Publications/PDF/PRR/2007/PRR-2007-04.pdf

[11] S. Y. Cheung, S. C. Ergen, B. Dundar, S. Ganesh, C.-W. Tan, and P. Varaiya, "Traffic Measurement and Vehicle Classification with a Single Magnetic Sensor," ser. 84th Annual Meeting. Washington D.C: Transport Research Board, January 2005. [Online]. Available: http://paleale.eecs.berkeley.edu/~varaiya/

[12] C. Johansson, C. Jonasson, and M. Erlandsson, "Magnetic Sensors for Traffic Detection," Imego AB, 411 33 Göteborg, Sweden, Tech. Rep. 110078-rapport, 2006.

[13] M. J. Caruso, T. Bratland, D. C. H. Smith, and R. Schneider, "A New Perspective on Magnetic Field Sensing," Honeywell SSEC and Nonvolatile Electronics Inc., Tech. Rep., 1998. [Online]. Available: http://www.ssec.honeywell.com

[14] *Smart Digital Magnetometer, HMR2300*, Honeywell International, Solid State Electronics Center. [Online]. Available: http://www.ssec.honeywell.com

[15] *Vehicle Detection Using AMR Sensors, Application Note AN218*, Honeywell International, Solid State Electronics Center. [Online]. Available: http://www.ssec.honeywell.com

[16] *1- and 2-axis Magnetic Sensors, HMC1001/1002, HMC1021/1022*, Honeywell International, Solid State Electronics Center. [Online]. Available: http://www.ssec.honeywell.com

[17] *Set/Reset Function for Magnetic Sensors, Application Note AN213*, Honeywell International, Solid State Electronics Center. [Online]. Available: http://www.ssec.honeywell.com

[18] W. J. Broad, "Will Compasses Point South?" *New York Times*, July 2004. [Online]. Available: http://www.nytimes.com

[19] D. K. Cheng, *Fundamentals of Engineering Electromagnetics*. Addison-Wesley Publishing Company, 1993.

[20] R. P. Feynman, R. B. Leighton, and M. Sands, *The Feynman Lectures on Physics, Mainly Electromagnetism and Matter*, 2nd ed. Reading, Massachusetts: Addison-Wesley Publishing Company, 1964.

[21] C. Nordling and J. Österman, *Physics Handbook for Science and Engineering*, 8th ed. Lund, Sweden: Studentlitteratur, April 2006.

[22] C. Johansson, C. Jonasson, and M. Erlandsson, "Traffic Detection System, Phase 2," Imego AB, 411 33 Göteborg, Sweden, Tech. Rep. 110078-rapport-projekt2, 2007.

[23] A. Behravan, "Evaluation and Compensation of Nonlinear Distortion in Multicarrier Communication Systems," Ph.D. dissertation, Chalmers University of Technology, Göteborg, Sweden, May 2006.

[24] C. Sun, "An Investigation in the Use of Inductive Loop Signatures for Vehicle Classification," California Partners for Advanced Transit and Highways, Research Report UCB-ITS-PRR-2000-4, March 2000.

[25] A. N. Knaian, "A Wireless Sensor Network for Smart Roadbeds and Intelligent Transportation Systems," Master's thesis, Massachusetts Institute of Technology, Boston, USA, May 2000.

[26] B. Coifman, S. Dhoorjaty, and Z.-H. Lee, "Estimating Median Velocity Instead of Mean Velocity at Single Loop Detectors," *Transportation Research Part C: Emerging Technologies*, 2003.

[27] B. Coifman, "Improved Velocity Estimation Using Single Loop Detectors," *Transportation Research*, 2001.

[28] L. Råde and B. Westergren, *Mathematics Handbook for Science and Engineering*. Lund, Sweden: Studentlitteratur, 2001.

[29] *3-axis Magnetic Sensor, HMC1043*, Honeywell International, Solid State Electronics Center. [Online]. Available: http://www.ssec.honeywell.com

Appendix A

Graphs

This appendix contains plots and figures that are to voluminous to be placed anywhere else.

A.1 Fast Fourier Transform of vehicle signatures

The sampling frequency in all figures in this section is 25 Hz. The of the simulated data FFT has been plotted for all vehicle types used in this thesis and for all three axes. The sensor was placed at the side of the road.

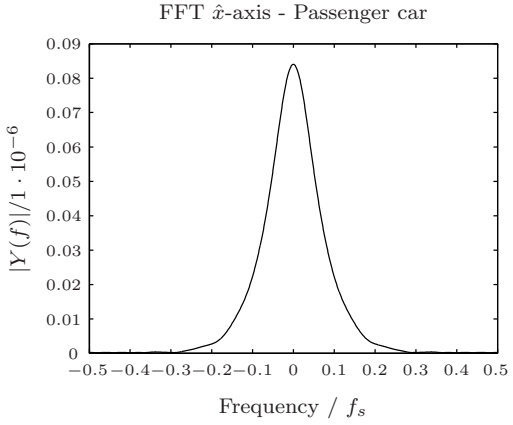

Figure A.1a: *FFT $\hat{x}$-axis - Passenger car.*

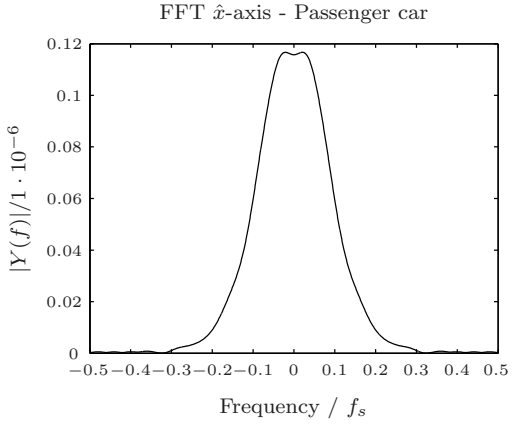

Figure A.1b: *FFT $\hat{x}$-axis - Another passenger car.*

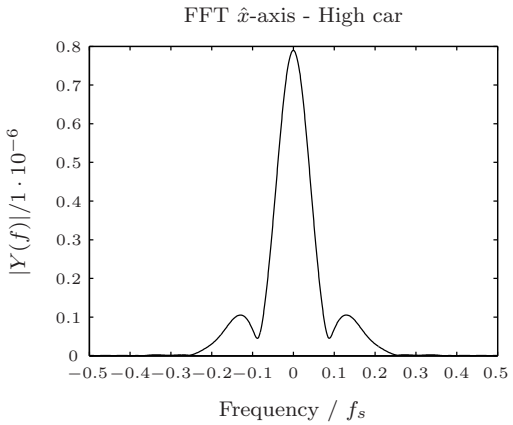

Figure A.1c: *FFT $\hat{x}$-axis - High car.*

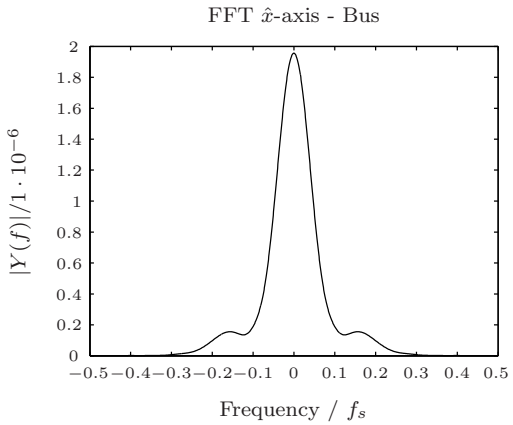

Figure A.1d: *FFT $\hat{x}$-axis - Bus.*

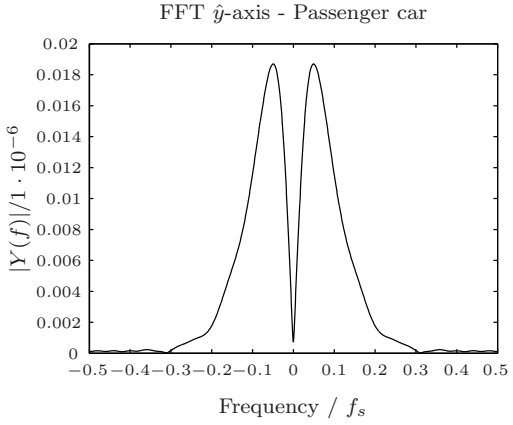

Figure A.2a: *FFT $\hat{y}$-axis - Passenger car.*

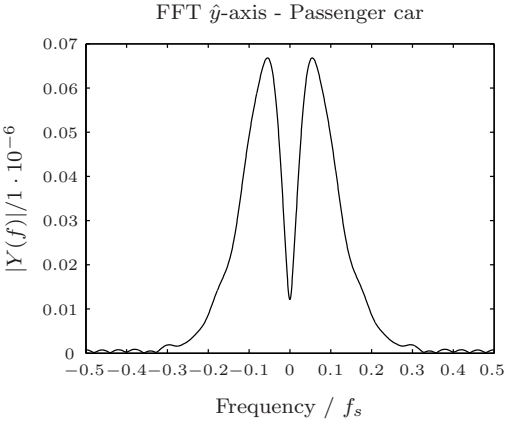

Figure A.2b: *FFT $\hat{y}$-axis - Another passenger car.*

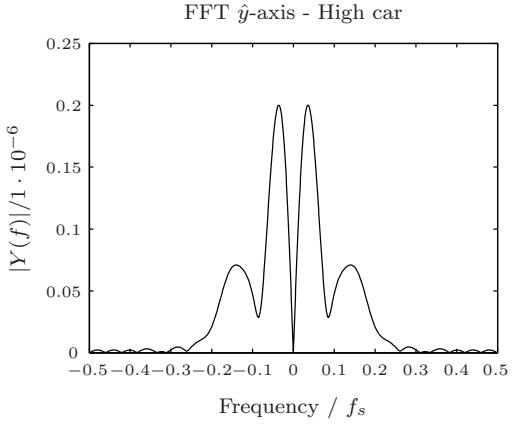

Figure A.2c: *FFT $\hat{y}$-axis - High car.*

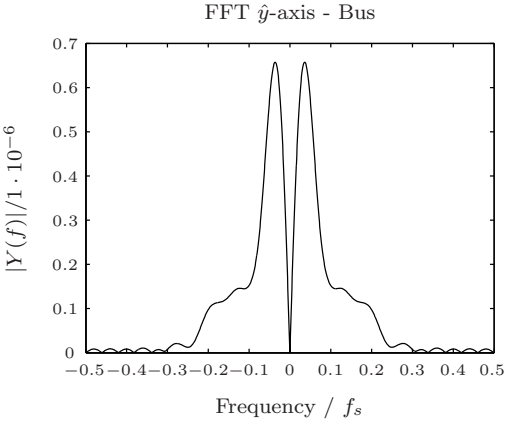

Figure A.2d: *FFT $\hat{y}$-axis - Bus.*

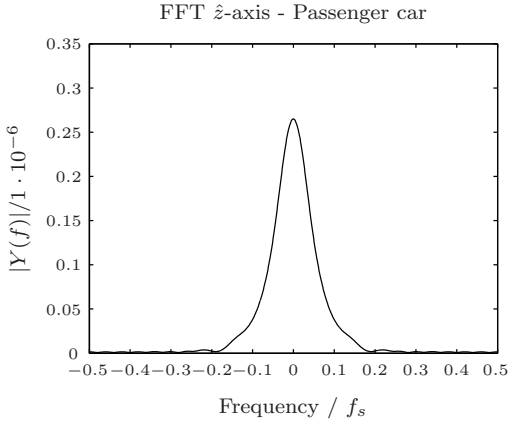

Figure A.3a: *FFT $\hat{z}$-axis - Passenger car.*

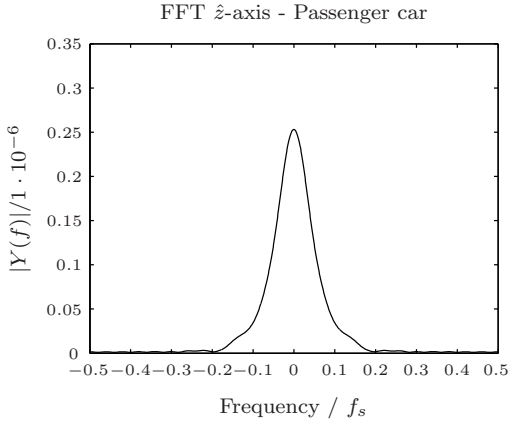

Figure A.3b: *FFT $\hat{z}$-axis - Another passenger car.*

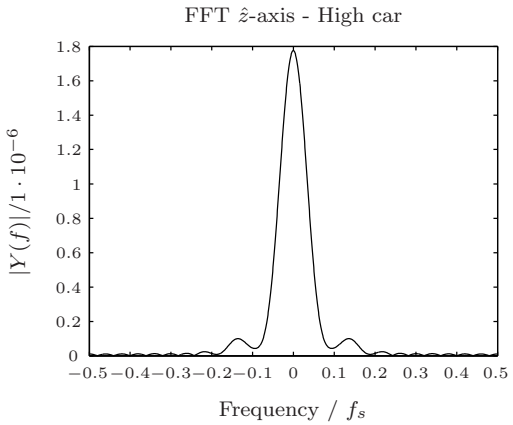

Figure A.3c: *FFT $\hat{z}$-axis - High car.*

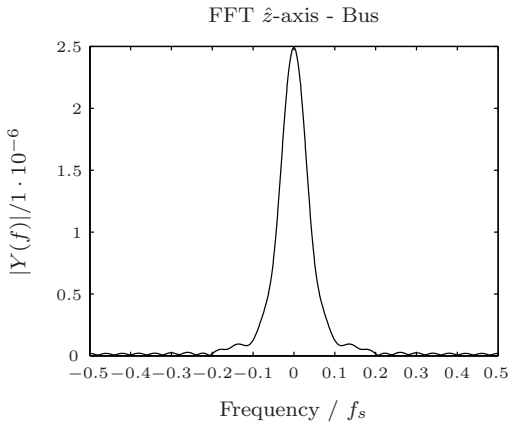

Figure A.3d: *FFT $\hat{z}$-axis - Bus.*

Appendix B

Simulator

The simulator is written in MATLAB and C with MEX-interface, and contains vehicle generator, traffic generator, sensor simulator, (network simulator), algorithms. It is built in modules and can easily be expanded to fit the application. The modular layout can be seen in Figure B.1.

There are a number of interfaces to the simulator, two of them can be seen in Figures B.2a and B.2b.

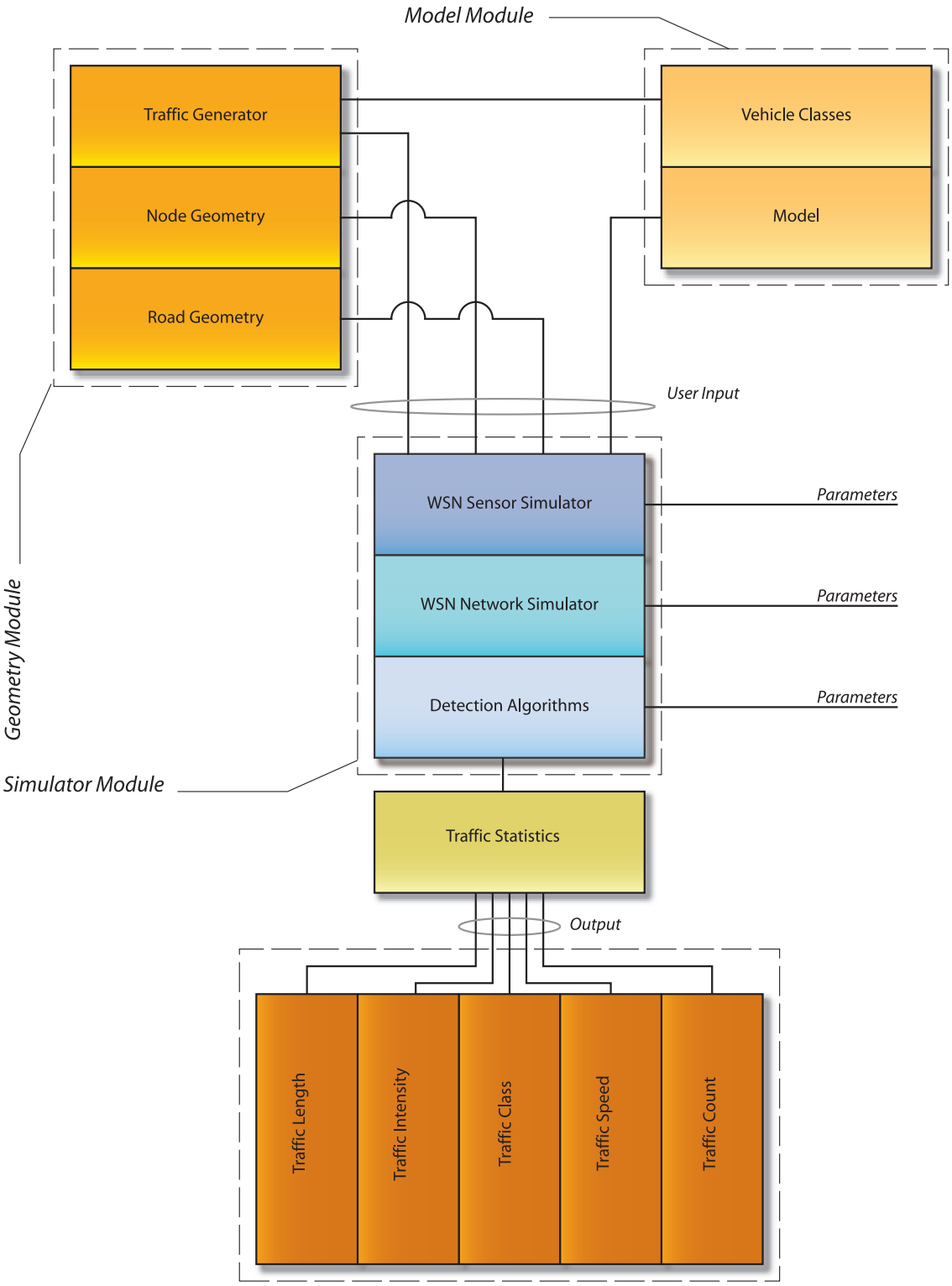

Figure B.1: *Simulator overview. Modules.*

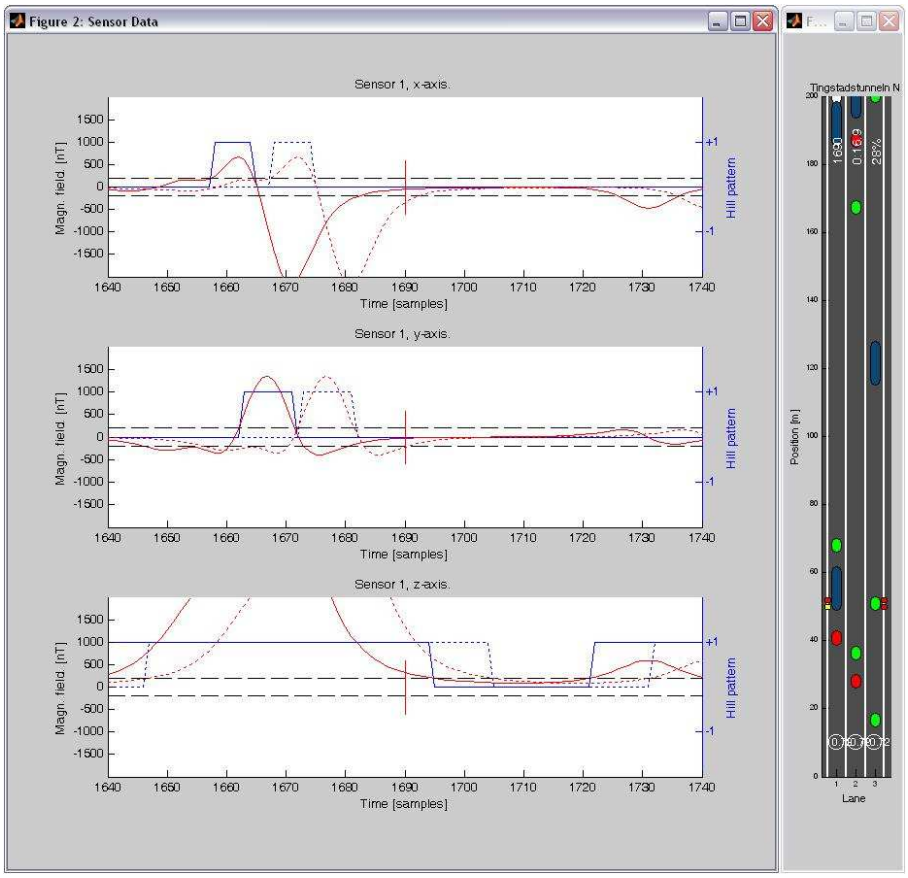

Figure B.2a: *Simple simulator interface in* MATLAB.

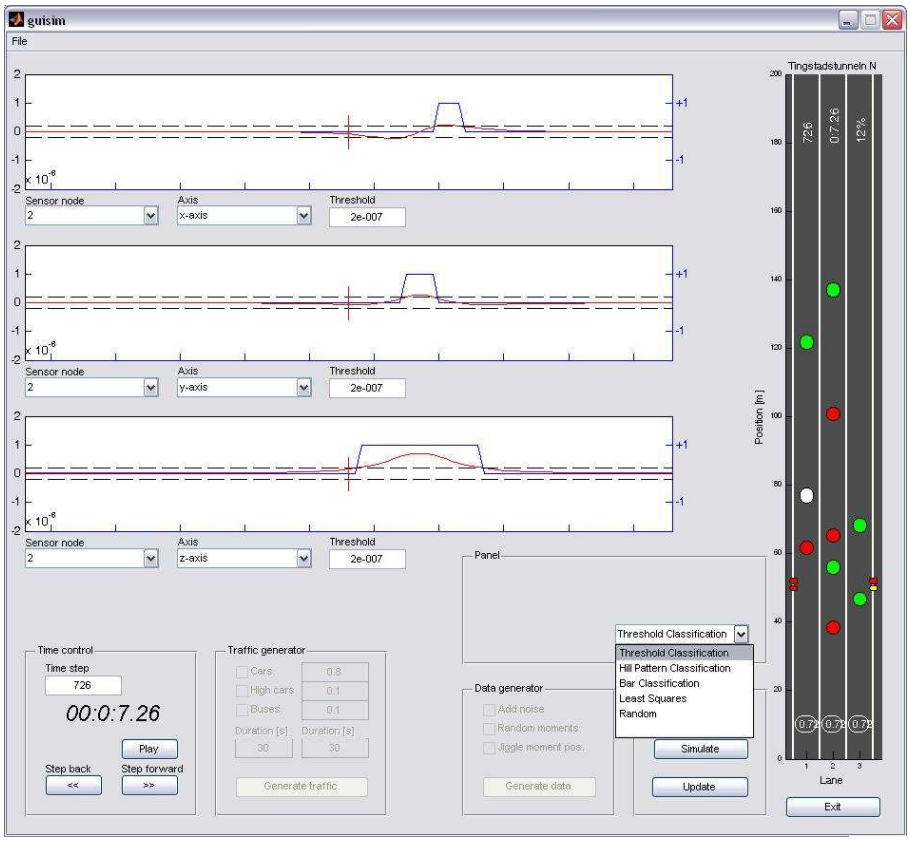

Figure B.2b: *Advanced simulator interface in* MATLAB.

Appendix C

Tables

The table herein illustrates the different sensor types used in this project.

Table C.1: *Honeywell AMR sensors*

Sensor	# Axis	Sens. [mV/V/mT]	Pwr supply	Field range [mT]	BW	Noise [nT/$\sqrt{\text{Hz}}$]	Op temp.	Price
HMC1043[29]	3	10	1.8–10 V	±0.6	5 MHz	0.8[a]	-40 – 125 ℃	$25 (1 pcs)
HMC1001[16]	1	32	5–12 V	±0.2	5 MHz		-55 – 150 ℃	$17 (10 pcs)
HMC1002[16]	2	32	5–12 V	±0.2	5 MHz		-55 – 150 ℃	$19 (10 pcs)
HMC2300[b][14]	3		6.5–15 V	±0.2			-40 – 85 ℃	

[a] IMEGO
[b] Contains HMC1001 and HMC1002

Appendix D

Illustrations

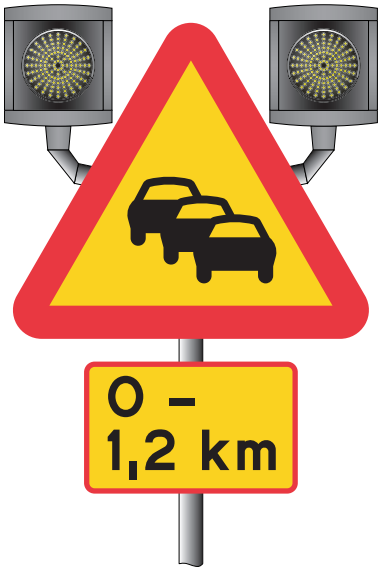

Figure D.1a: *Addition to old sign.*

Figure D.1b: *Proposed new sign.*

Figure D.1c: *Sign with Amparo SeeMe™ Main Unit.*

Index